Low-lying collective states in N≈40 nuclei in nuclear-DFT-based quadrupole collective Hamiltonian

Kouhei Washiyama (CCS, Univ. Tsukuba, Japan)

筑波大学
計算科学研究センター
Center for Computational Sciences

Collaborator: Kenichi Yoshida (RCNP, Osaka Univ., Japan)

Spectroscopy in neutron-rich N=40 nuclei

Five-dimensional collective Hamiltonian

Analysis in N=40 nuclei

Excited 0+ state

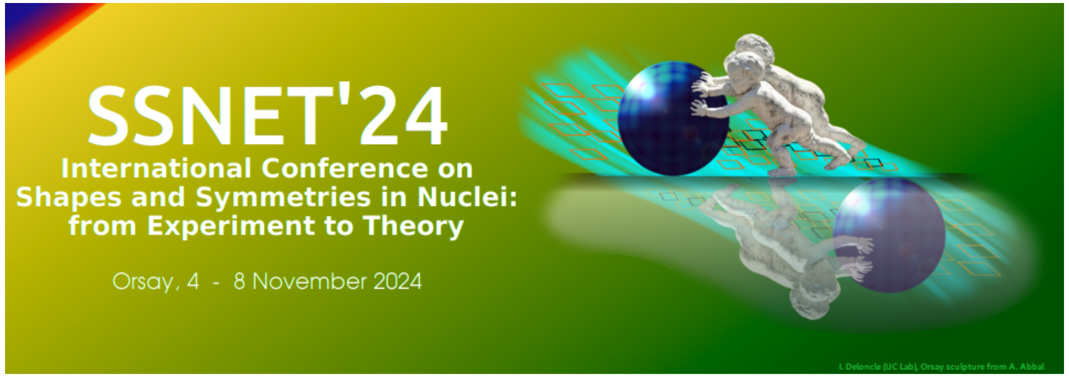

Spectroscopy in neutron-rich N=40 nuclei

M.L. Cortés et al., PLB 800, 135071 (2020)

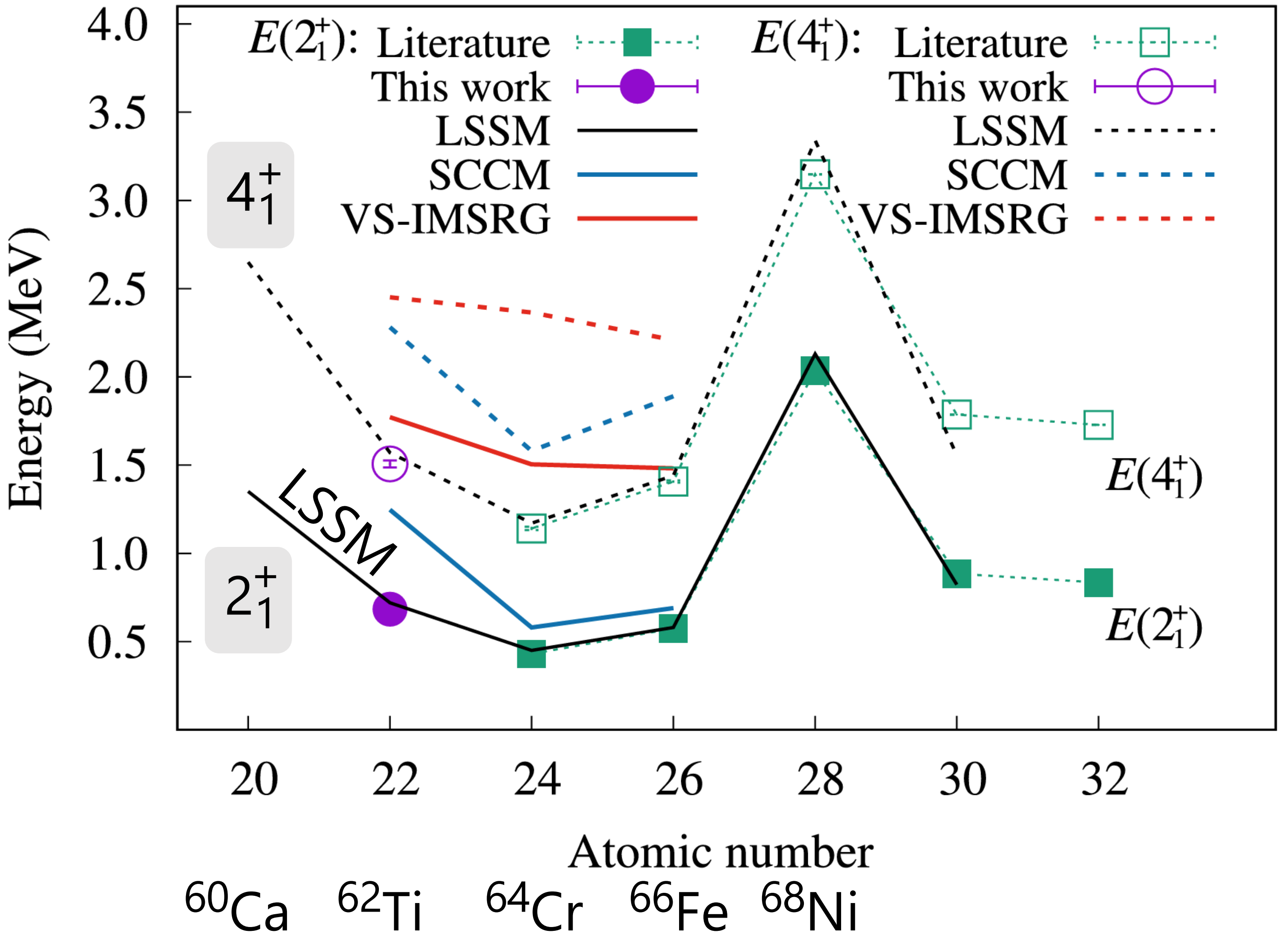

Increase of $E(2_1^+)$ in ^{62}Ti

LSSM (large-scale shell model)

S.M. Lenzi, et al., PRC82(2010)054301

$^{62,\,64}$Cr

A. Gade et al., PRC103, 014314 (2021)

Spectroscopy toward ^{60}Ca

Shape coexistence, Shape fluctuation

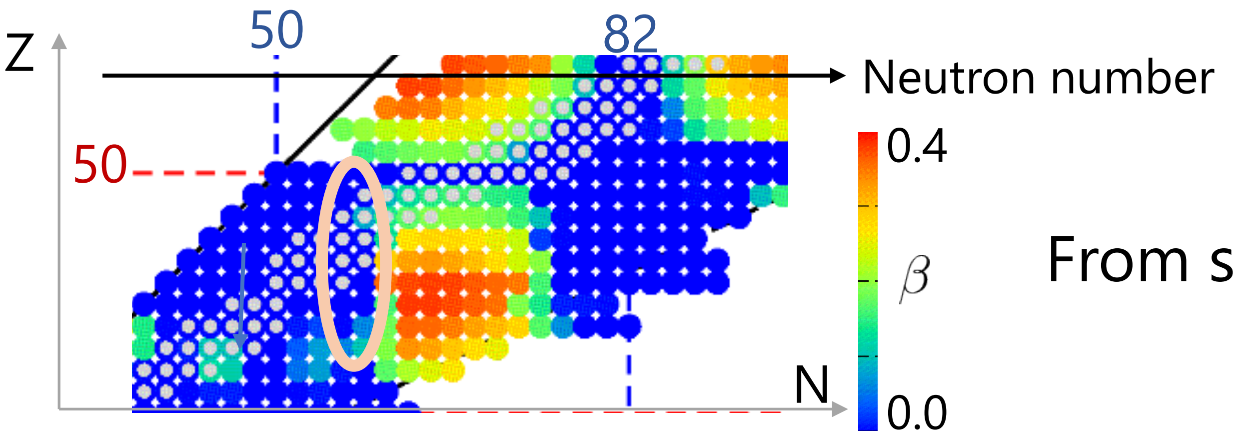

Figure taken from Ebata, Nakatsukasa, Phys. Scr. 92 (2017) 064005

From spherical to deformed nuclei

Shape fluctuation

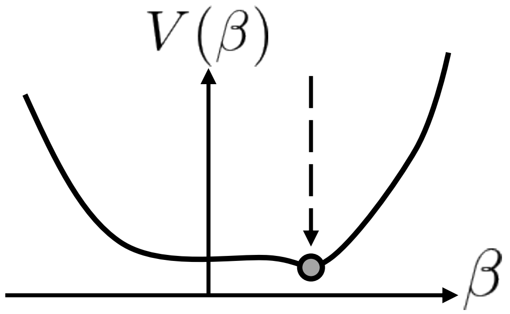

Shape coexistence

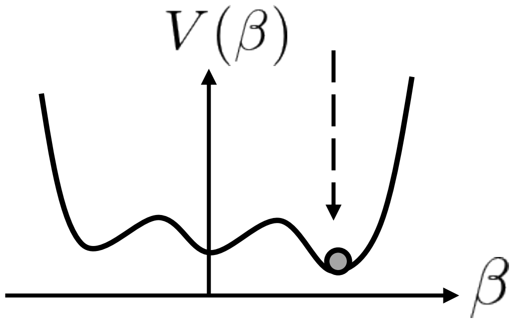

Mean-field description is not enough

Description beyond mean field is necessary

"Dynamical" shape coexistence?

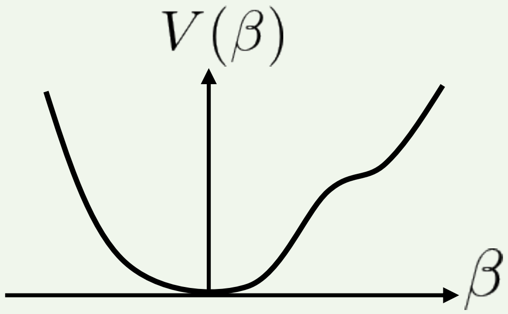

Correlation beyond mean field generates low 0^+ states

Purpose of the present work

To describe low-lying states in N=40 nuclei by using a model beyond mean field to treat large-amplitude shape fluctuation

Quadrupole collectivity and beyond-mean-field approach

Five-dimensional collective Hamiltonian (5DCH) method

$$\mathcal{H} = T_{\mathrm{vib}} + T_{\mathrm{rot}} + V(\beta,\gamma)$$

Vibrational mass

$$T_{\mathrm{vib}} = \frac{1}{2}D_{\beta\beta}(\beta,\gamma)\dot{\beta}^2 + D_{\beta\gamma}(\beta,\gamma)\dot{\beta}\dot{\gamma} + \frac{1}{2}D_{\gamma\gamma}(\beta,\gamma)\dot{\gamma}^2$$

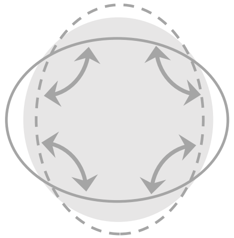

$$T_{\mathrm{rot}} = \frac{1}{2}\sum_{k=1}^{3}\mathcal{J}_k(\beta,\gamma)\omega_k^2$$

Moment of inertia

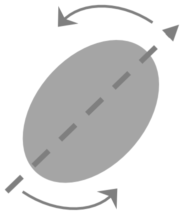

Inertia ⟺ Quadrupole collectivity

Quantize Hamiltonian

$$\hat{H}\Psi_{\alpha IM}(\beta,\gamma,\Omega) = E_{\alpha I}\Psi_{\alpha IM}(\beta,\gamma,\Omega)$$

▼

$E_{\alpha I}$, transition probability B(E2)

5DCH based on nuclear DFT

Prochniak et al., NPA730 (2004) 59;

Niksic et at., PRC79 (2009) 034303;

Delaroche et al., PRC81 (2010) 014303, etc.

Calculation set up for the CHFB + LQRPA

$$\mathcal{H} = T_{\rm vib} + T_{\rm rot} + V(\beta,\gamma)$$

$$T_{\rm vib} = \frac{1}{2}D_{\beta\beta}(\beta,\gamma)\dot{\beta}^2 + D_{\beta\gamma}(\beta,\gamma)\dot{\beta}\dot{\gamma} + \frac{1}{2}D_{\gamma\gamma}(\beta,\gamma)\dot{\gamma}^2$$

$$T_{\rm rot} = \frac{1}{2}\sum_{k=1}^{3}\mathcal{J}_k(\beta,\gamma)\omega_k^2$$

$V(\beta,\gamma)$ Potential energy surface in the β–γ plane

Constrained HFB in three-dimensional coordinate

Skyrme SkM*, volume pairing, box size (23.2 fm)^3

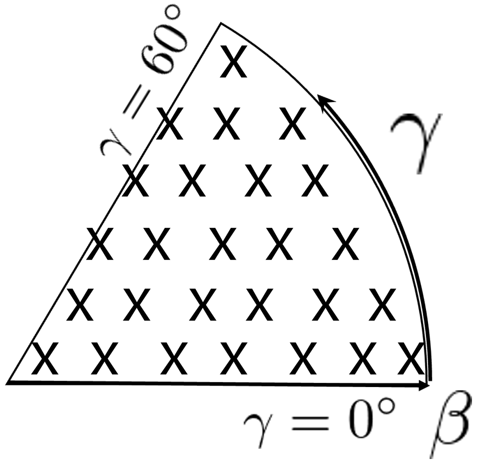

$D_{\beta\beta},\ D_{\beta\gamma},\ D_{\gamma\gamma},\ \mathcal{J}_k$ Inertial functions

Local QRPA with Skyrme DFT on each β,γ deformation

Improved description for the inertial functions

Washiyama, Hinohara, Nakatsukasa, Phys. Rev. C 109, L051301(2024)

0 < β < 0.6

0 < γ < 60°

~100 mesh points

Local QRPA

Hinohara et al., PRC82(2010)064313, PRC84(2011)061302; 85(2012)024323
Sato, Hinohara, NPA849 (2011) 53
Yoshida, Hinohara, PRC83 (2011) 061302

Result: potential energy surface in N=40 isotones

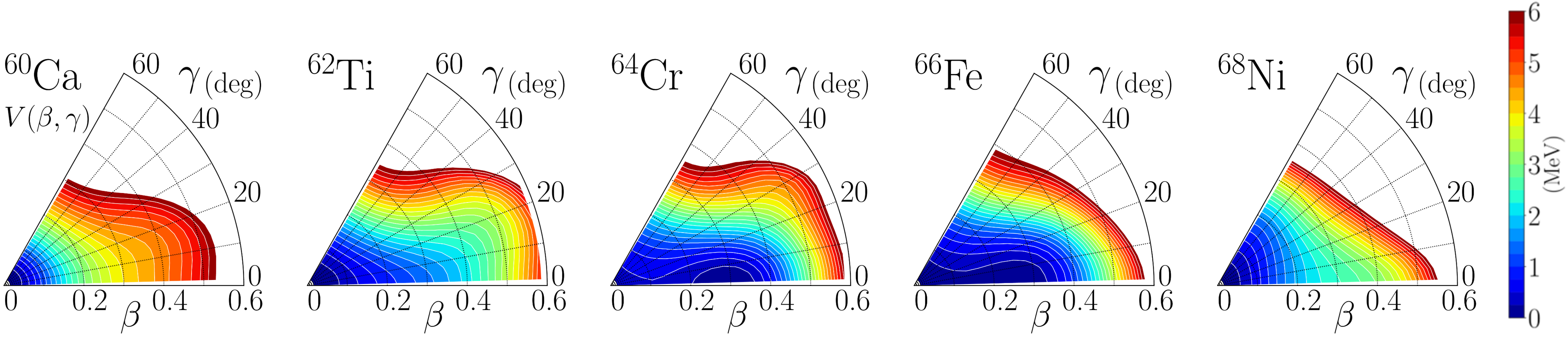

Z=20 Z=22 Z=24 Z=26 Z=28

Mean-field level, Spherical → Prolate → Spherical

SkM*
Volume pairing

Washiyama & Yoshida, in preparation

Systematics on the 2_1 energy in N=40

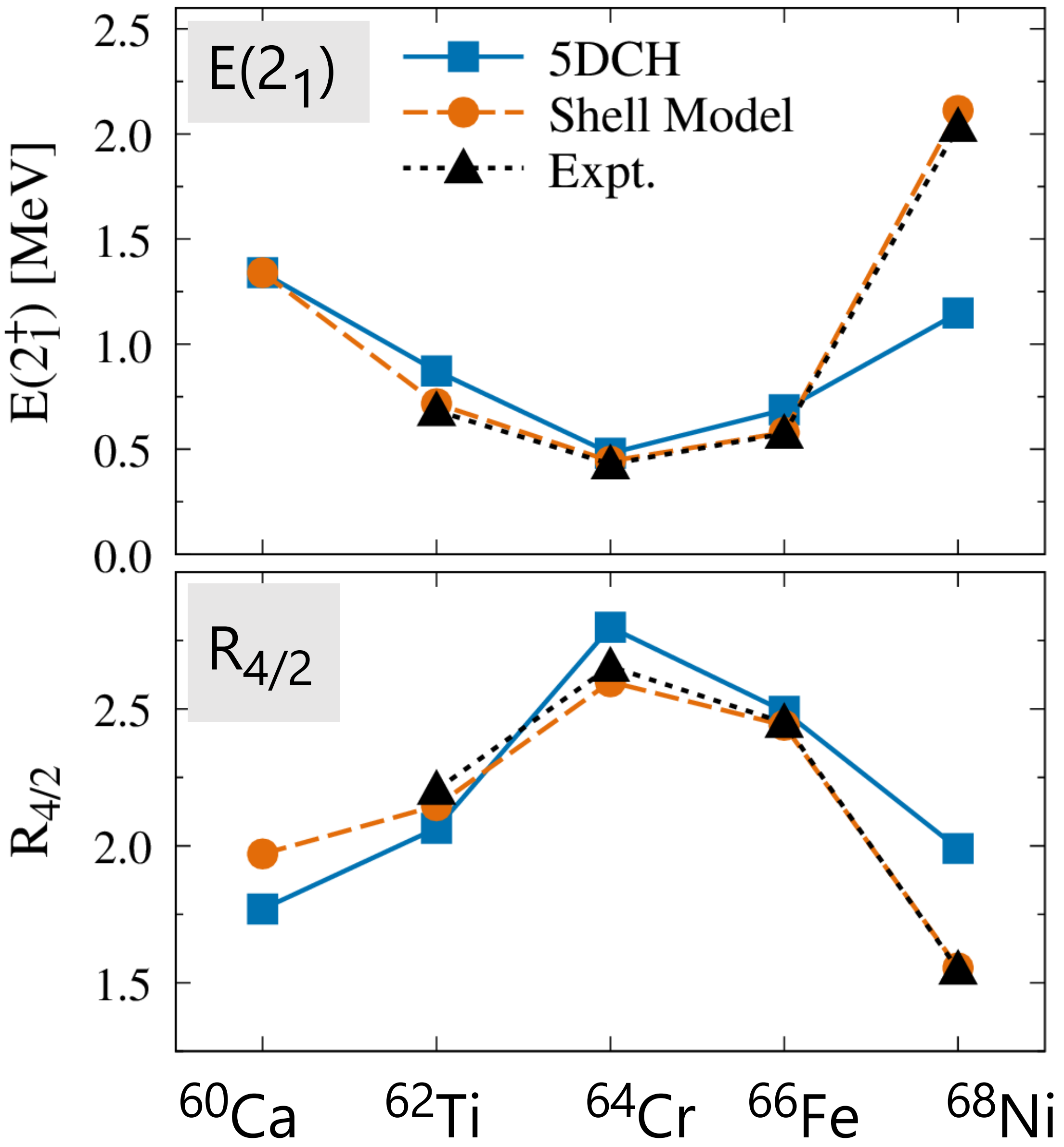

5DCH: five-dimensional collective Hamiltonian

Shell model : Lenzi et al., PRC82,054301 (2010)

Good on energy and $R_{4/2} = E(4_1)/E(2_1)$

Large deviation in ^{68}Ni

(good description by shell model)

Shell model space

Proton: pf shell

Neutron: 0f5/2, 1p3/2, 1p1/2, 0g9/2, 1d5/2

Washiyama & Yoshida, in preparation

Systematics on B(E2) in N=40

B(E2): Reduced transition probability

$$B(E2; 2_1^+ \to 0_1^+) = |\langle 2_1^+ || \hat{Q}_2 || 0_1^+ \rangle|^2 / 5$$

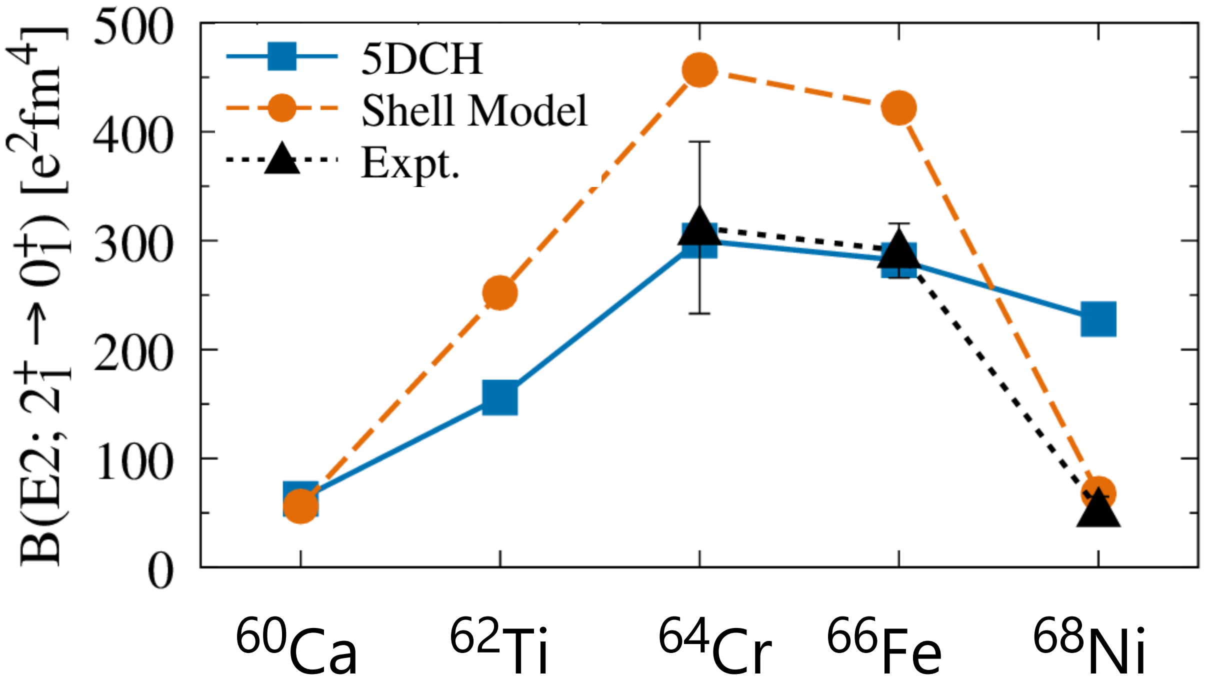

Good in ^{64}Cr, ^{66}Fe

Large deviation in ^{68}Ni

(good description by shell model)

Discussion: Quadrupole collectivity in ^{60}Ca

Potential

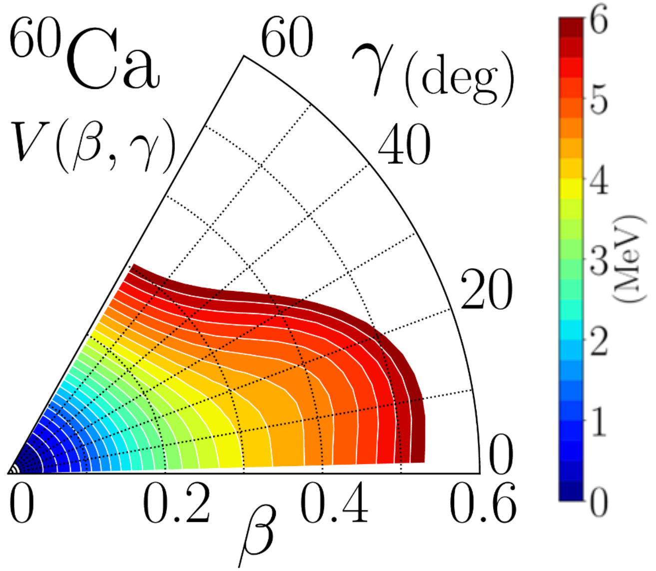

Squared vibrational wave functions $\beta^4\sqrt{W(\beta,\gamma)R(\beta,\gamma)}|\Phi_{\alpha I}(\beta,\gamma)|^2$

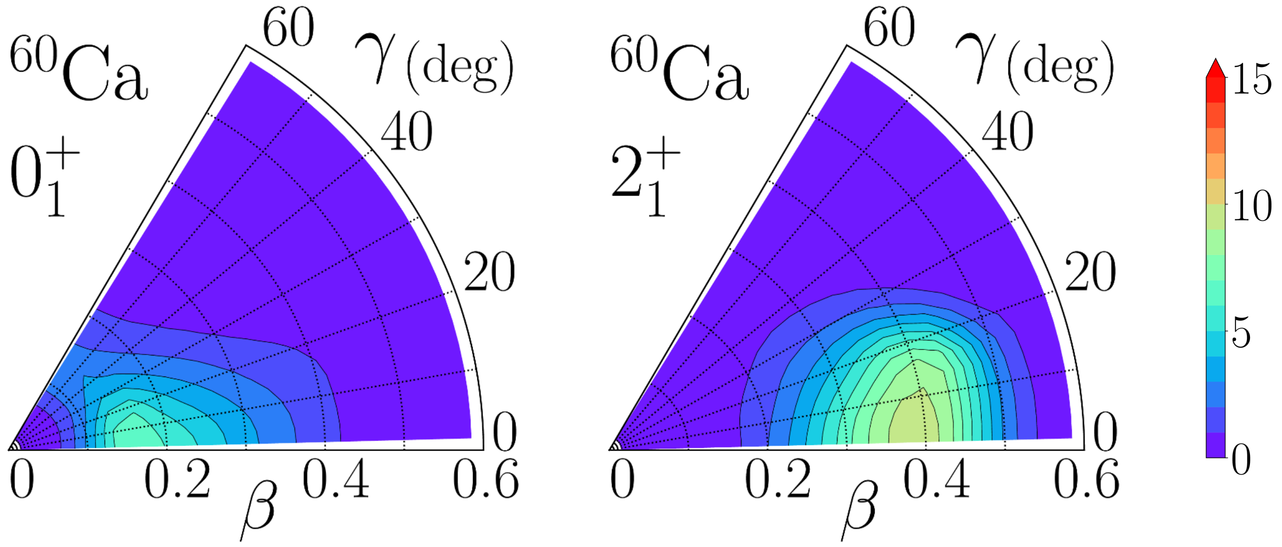

Wave functions spread over large β

➡ Large quadrupole collectivity ➡ **Breaking of N=40 magicity**

Shell model: 4p-4h excitation (~60%) across the N=40 gap

High quadrupole collectivity

Lenzi et al., PRC82,054301 (2010)

Discussion: low-lying 0_2 state in N=40 isotones

$R_{0/2} = E(0_2) / E(2_1)$

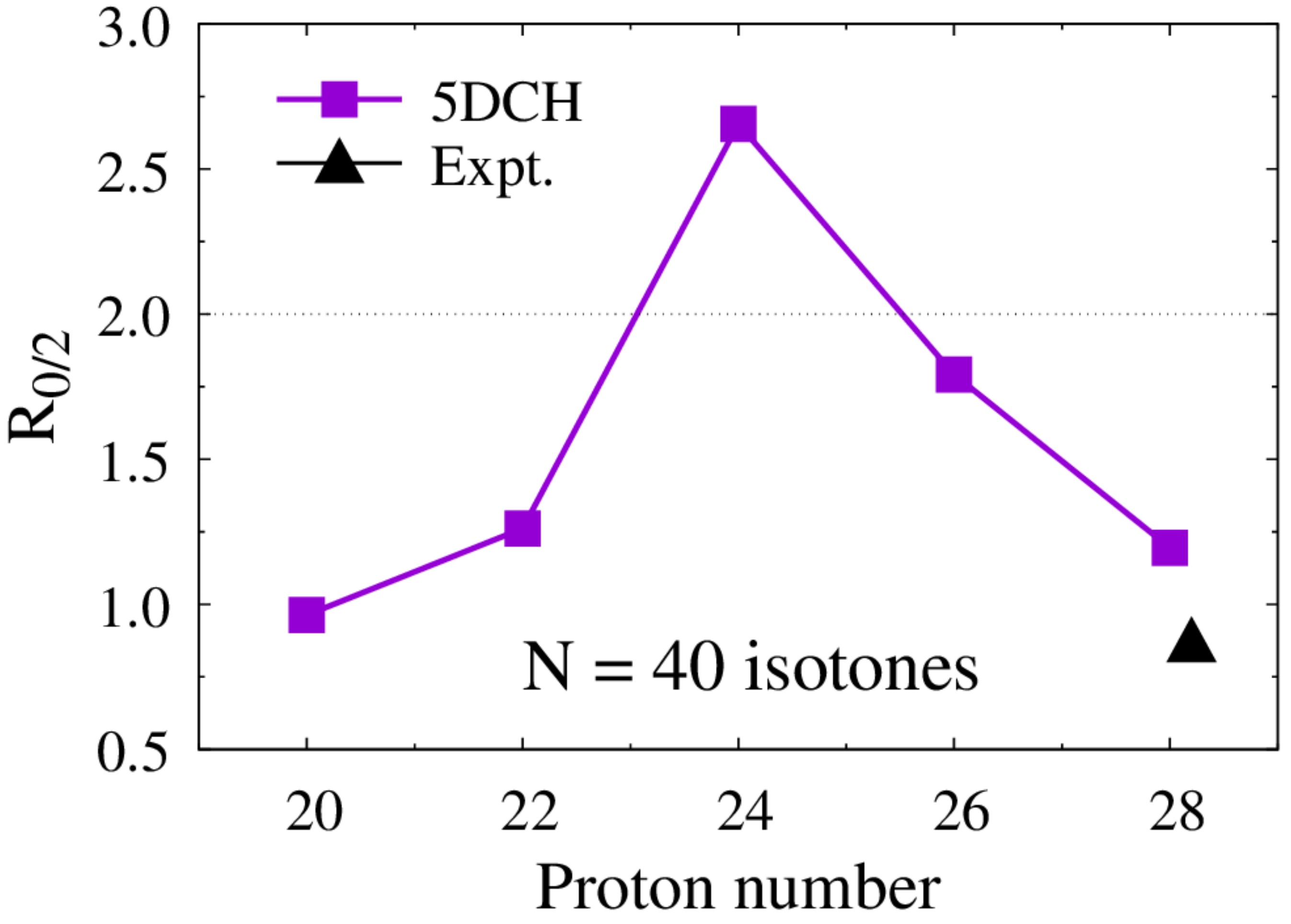

^{60}Ca ^{62}Ti ^{64}Cr ^{66}Fe ^{68}Ni

^{60}Ca $R_{0/2} = 0.96$

^{68}Ni $R_{0/2} = 1.19$

Spherical vibrator
$R_{0/2} = 2.0$

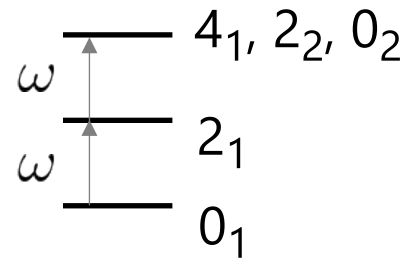

What is the origin of **low $R_{0/2}$** in ^{60}Ca, ^{68}Ni ?

Discussion: Role of inertial functions in the 0_2 state

Potential (axial shape)

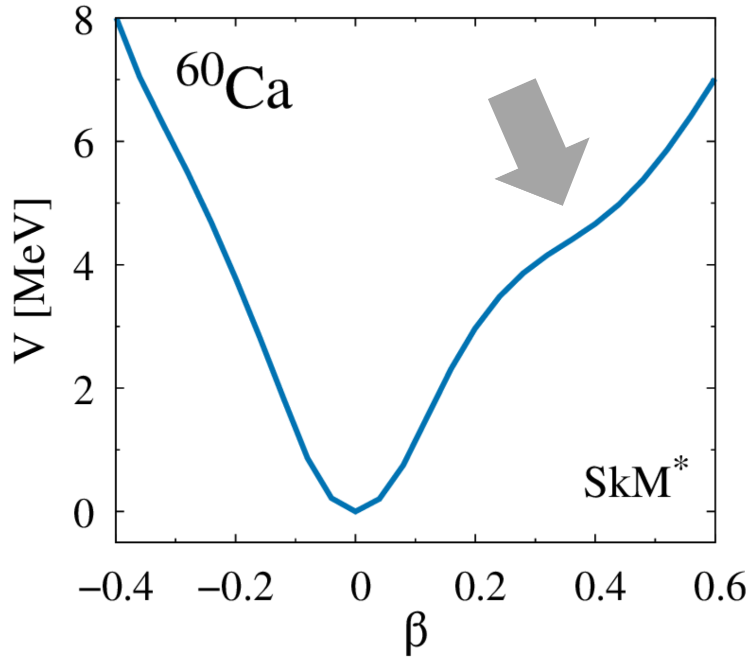

Spherical vibrator

Constant mass: ignore β–γ dependence

$$D_{\beta\beta}(\beta,\gamma) = D_{\gamma\gamma}(\beta,\gamma)/\beta^2 = D, \quad D_{\beta\gamma} = 0$$
$$D_1(\beta,\gamma) = D_2(\beta,\gamma) = D_3(\beta,\gamma) = D$$
$$\mathcal{J}_k(\beta,\gamma) = 4\beta^2 \sin^2(\gamma - 2\pi k/3)\, D_k(\beta,\gamma)$$

D is determined by fitting 2_1 energy

	Local QRPA	Constant
$R_{0/2}$ =	0.96	1.75

Low R0/2 ratio is not induced by the potential but induced by the dynamical correlations associated with the inertial functions in the kinetic energy.

Dynamical shape coexistence

Discussion: Role of shoulder in the potential

0_2^+ wave functions

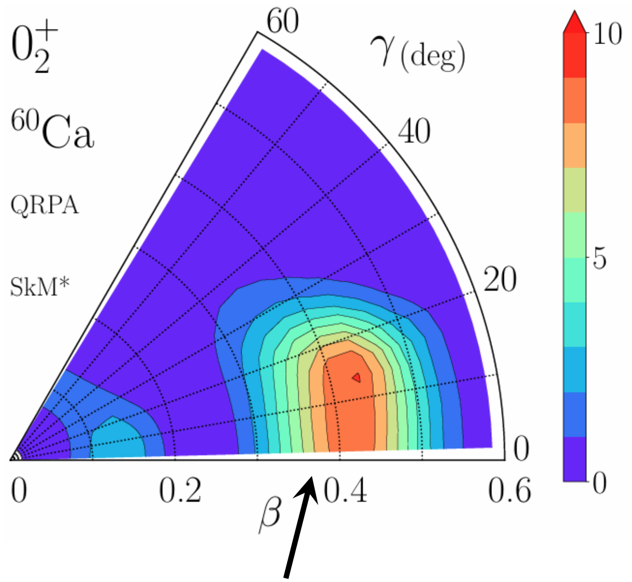

Large component

A shoulder in the potential affects $R_{0/2}$ ratio ?

Analytic potential

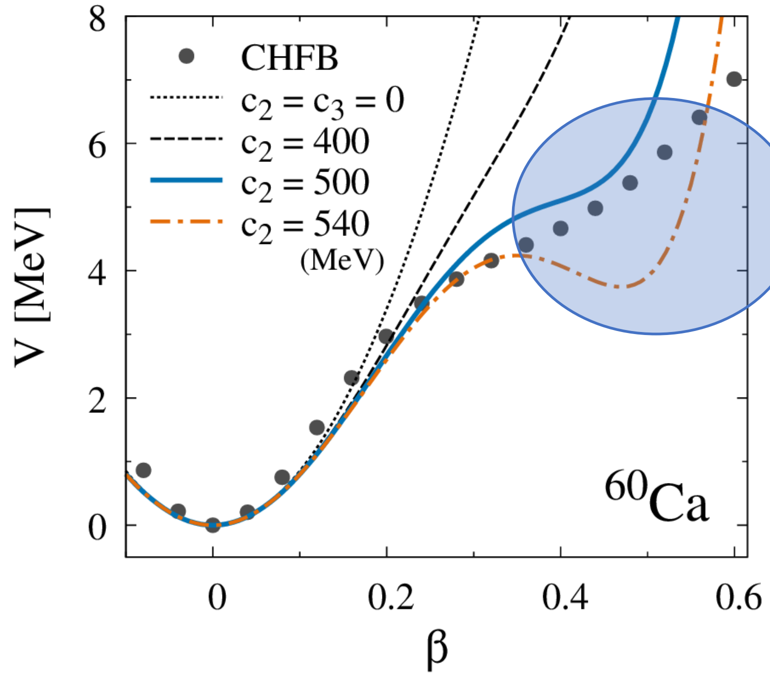

$$V(\beta,\gamma) = \frac{1}{2}c_1\beta^2 - c_2\beta^4 + c_3\beta^6$$

Energy ratio

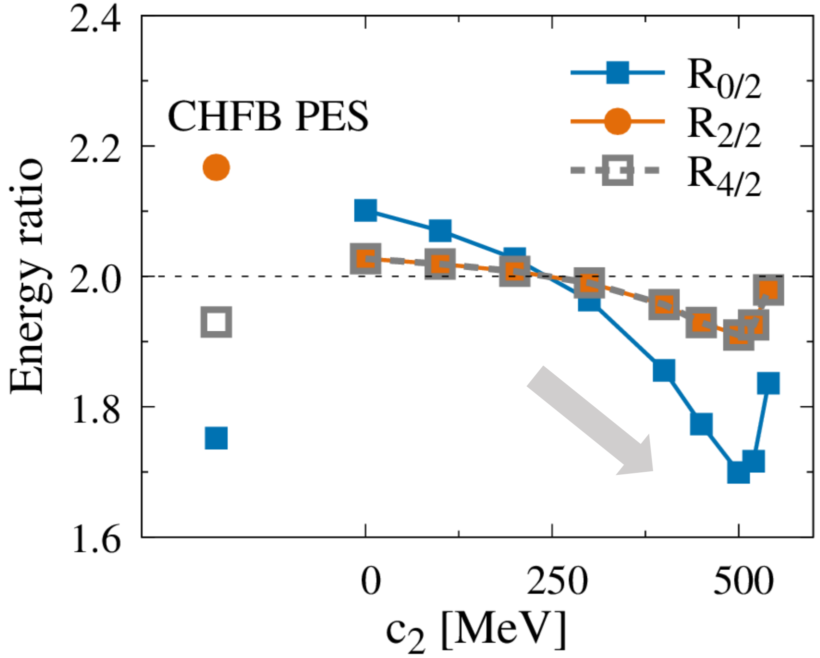

The shoulder decreases $R_{0/2}$ ratio

Dynamical shape coexistence (V + kinetic energy) induces low $R_{0/2}$

Summary

Neutron-rich N=40 isotones from ^{60}Ca to ^{68}NI

Collective Hamiltonian method beyond mean field

Good description in $E(2_1^+)$

Second 0^+ state in ^{60}Ca and ^{68}NI

- Dynamical shape coexistence (low kinetic energy and shoulder in PES) makes $R_{0/2}$ low
- Correlation beyond mean field generates low 0_2^+ state

This research used computational resources of OFP & Wisteria/BDEC-01 Odyssey (Univ. Tokyo), provided by the Multidisciplinary Cooperative Research Program in CCS, Univ. Tsukuba.

Vibrational kinetic energy to the 0_2 state

$$\langle \hat{T}_{\mathrm{vib}} \rangle = \iint d\beta d\gamma |G(\beta,\gamma)|^{1/2} \sum_{K=\mathrm{even}} \Phi^*_{IK\alpha}(\beta,\gamma)\hat{T}_{\mathrm{vib}}\Phi_{IK\alpha}(\beta,\gamma)$$

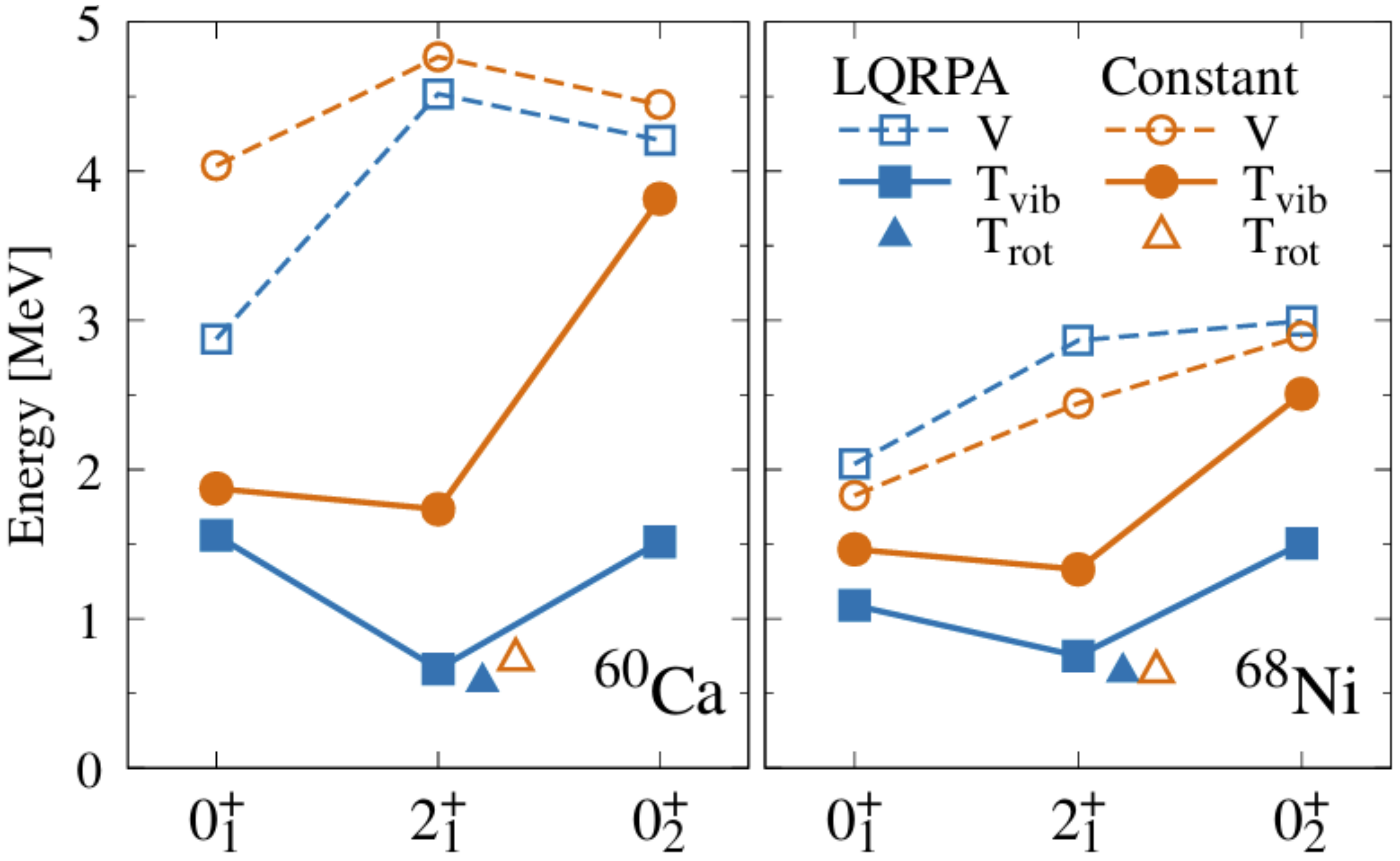

Vibrational wave functions in 60Ca

LQRPA inertial functions

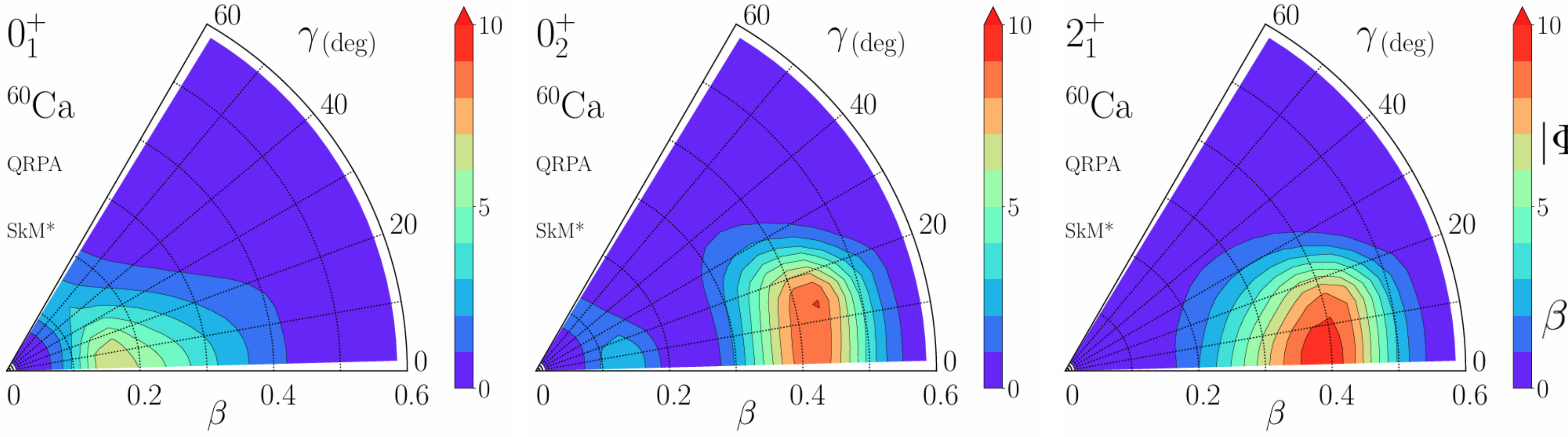

$$|\Phi_{\alpha I}(\beta,\gamma)|^2 = \sum_K |\Phi_{\alpha IK}(\beta,\gamma)|^2$$

$$\beta^4\sqrt{W(\beta,\gamma)R(\beta,\gamma)}|\Phi_{\alpha I}(\beta,\gamma)|^2$$

Constant mass

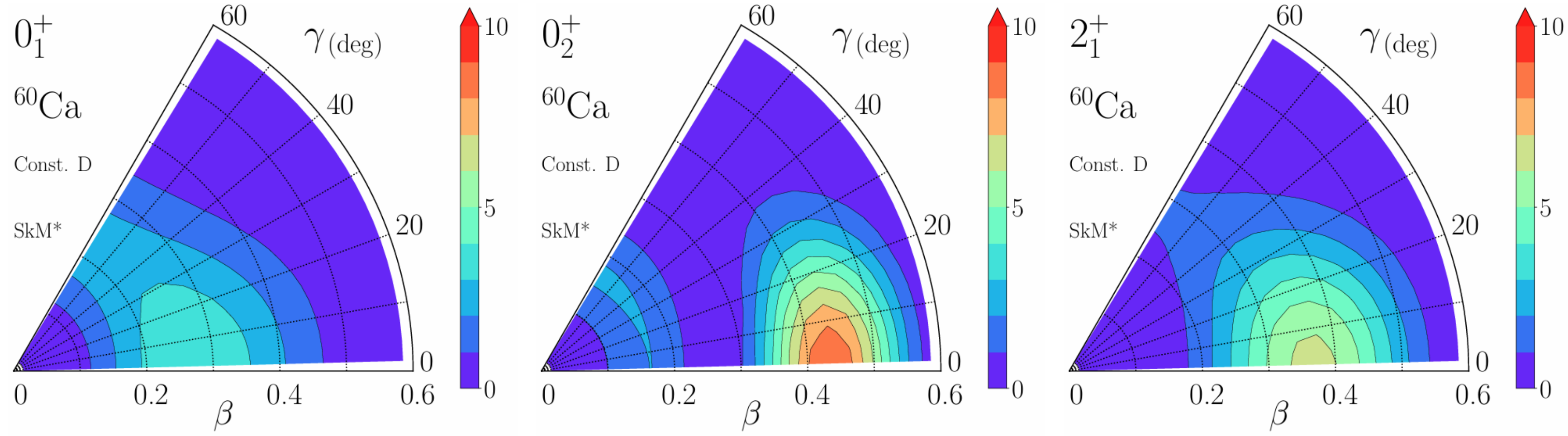

Inertial functions: LQRPA vs. Cranking approx.

Ratio of LQRPA to Cranking

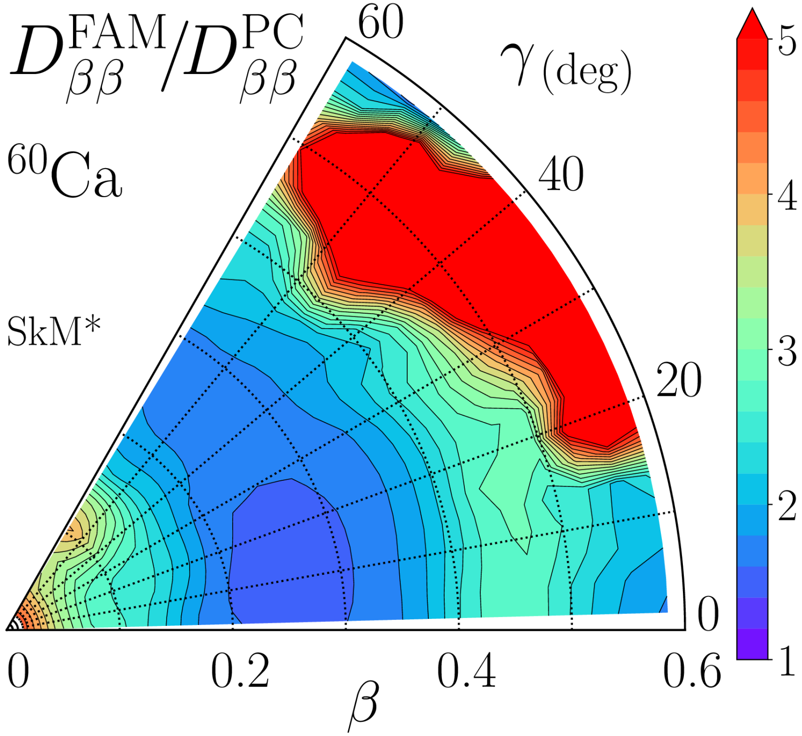

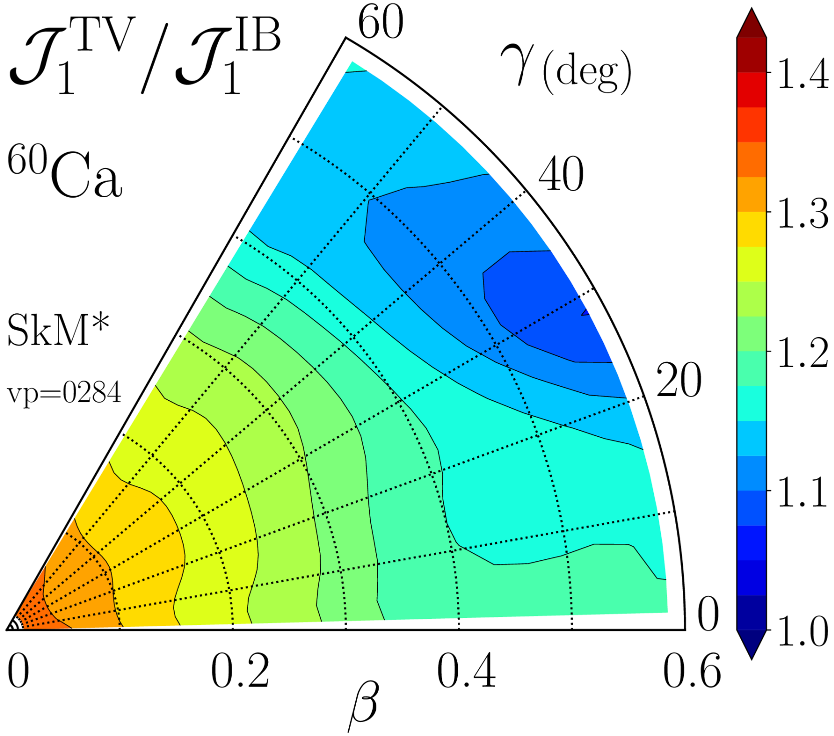

LQRPA inertial functions

Vibrational mass, 60Ca

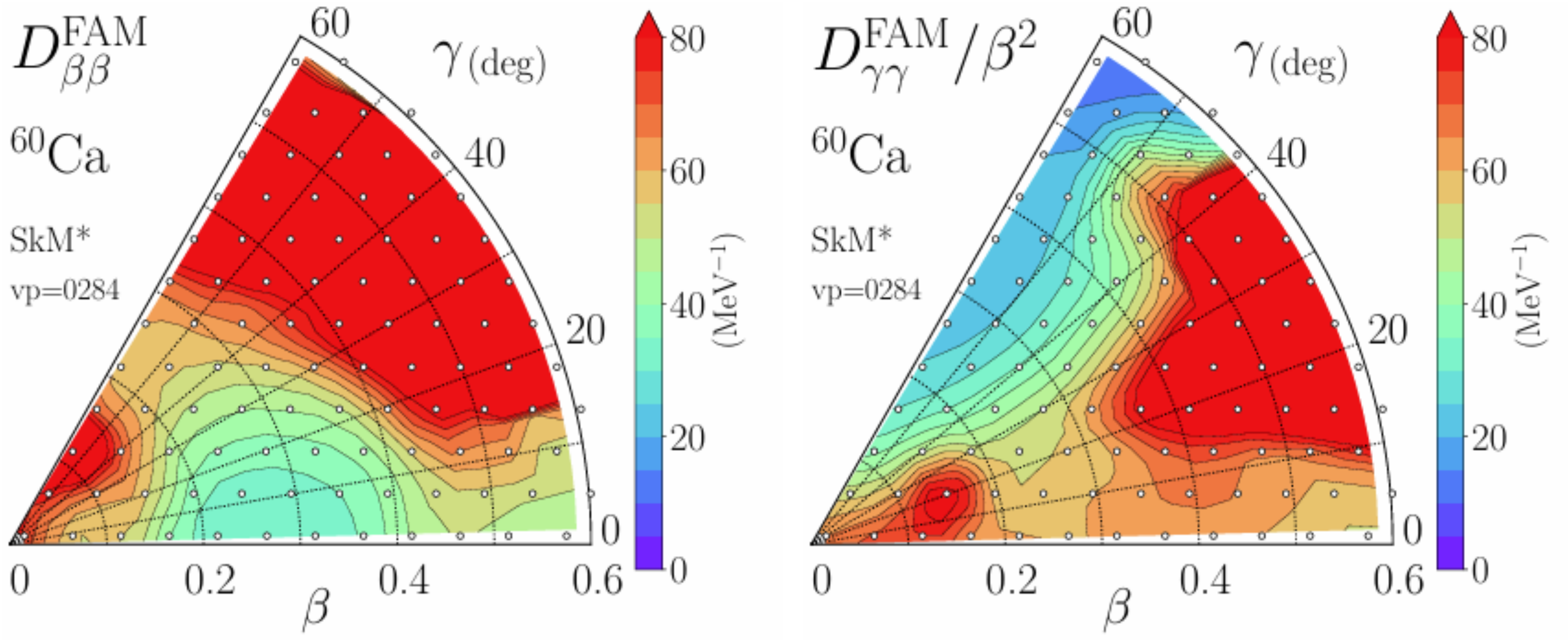

Vibrational kinetic energy to the 0_2 state

$$\langle \hat{T}_{\rm vib} \rangle = \iint d\beta d\gamma |G(\beta,\gamma)|^{1/2} \sum_{K=\rm even} \Phi^*_{IK\alpha}(\beta,\gamma)\hat{T}_{\rm vib}\Phi_{IK\alpha}(\beta,\gamma)$$

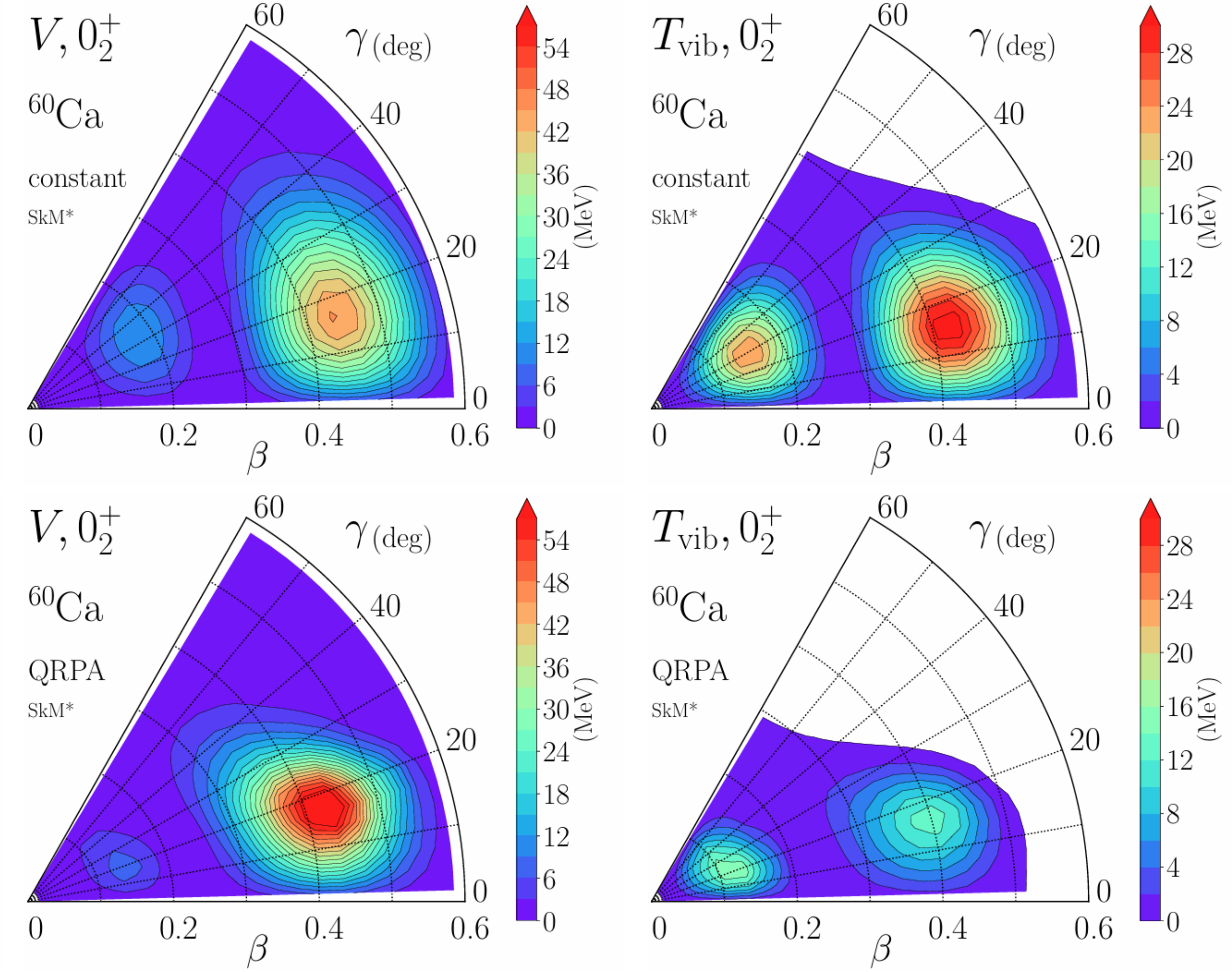

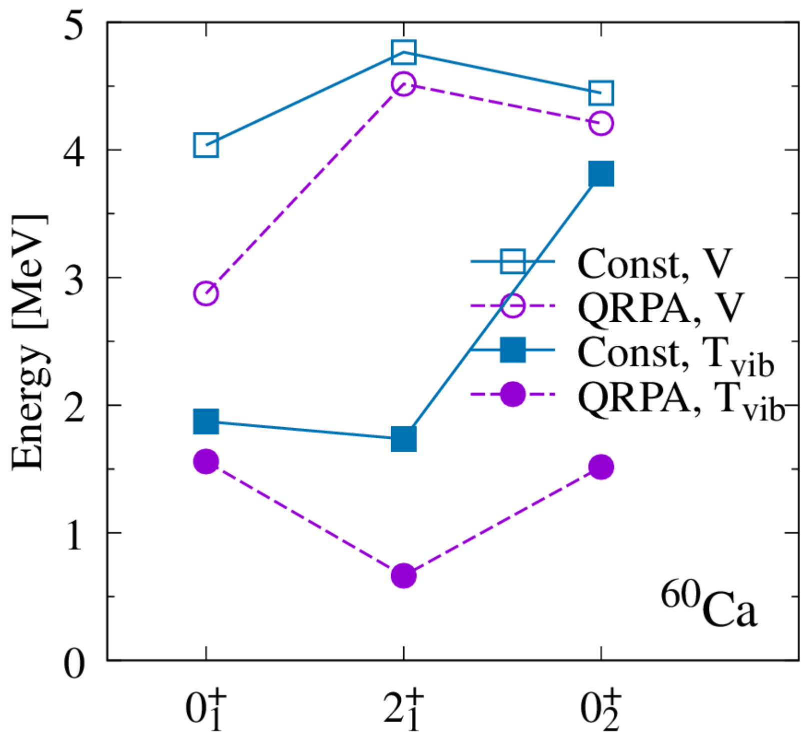

Low 0_2 energy and dynamical shape coexistence

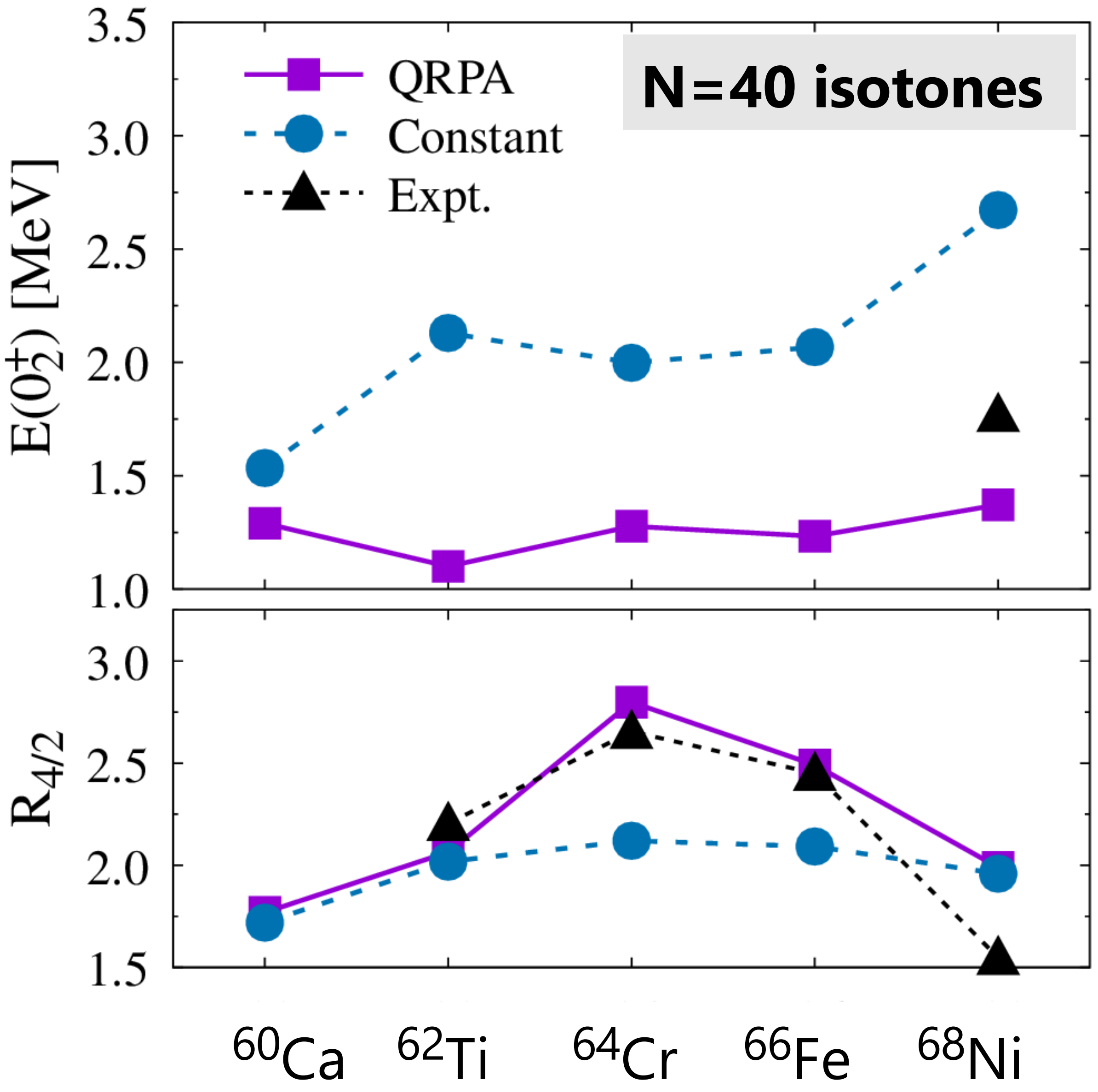

Significant decrease from constant $E(0_2)$ to QRPA $E(0_2)$

Dynamical shape coexistence

Potential + inertial functions

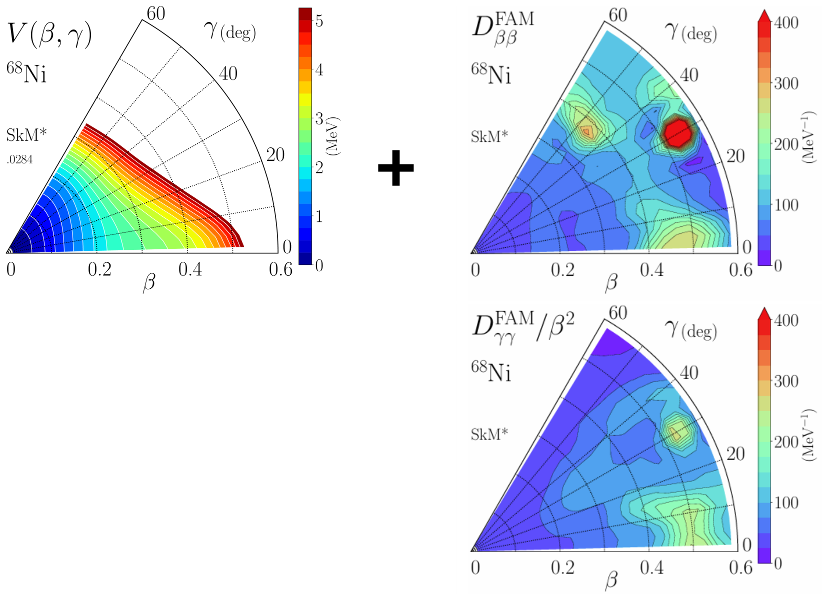

Low 0^+ energy

Positive-parity low-lying spectra in ^{64}Cr

^{64}Cr (N=40)

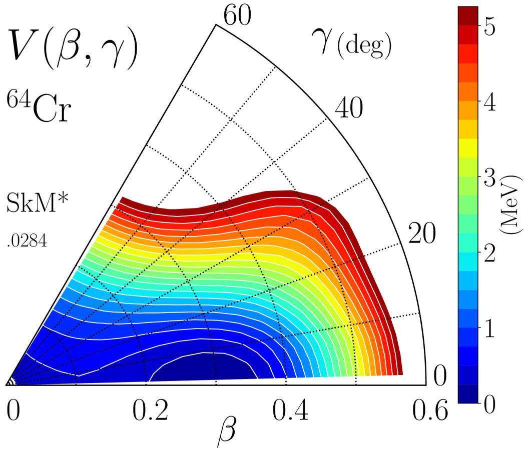

Cranking

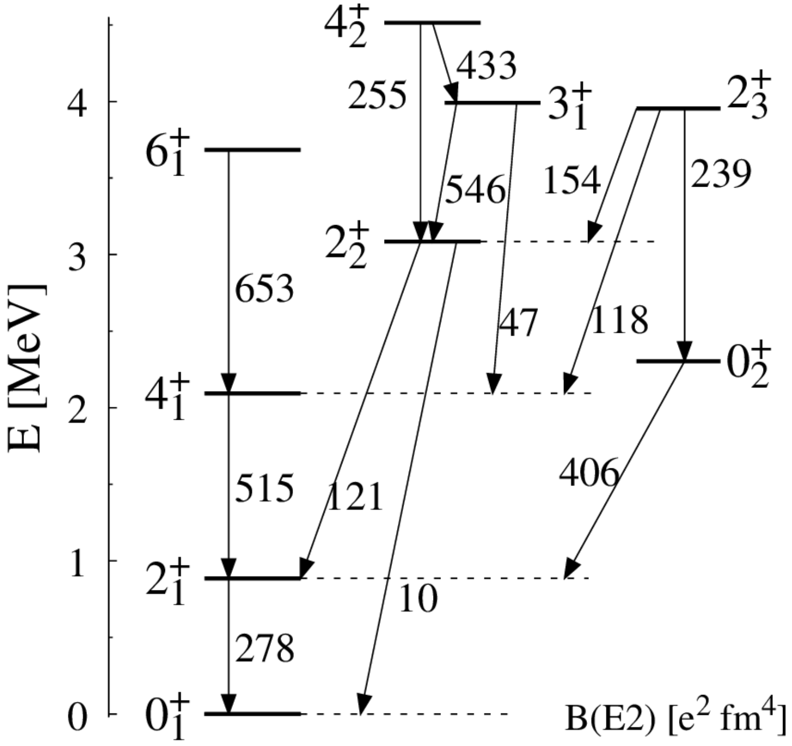

QRPA

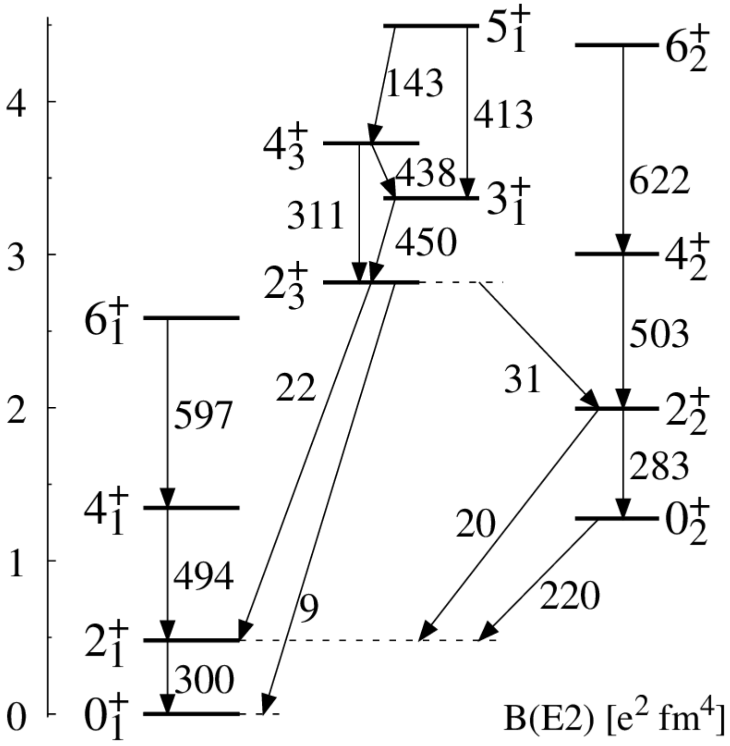

Expt.

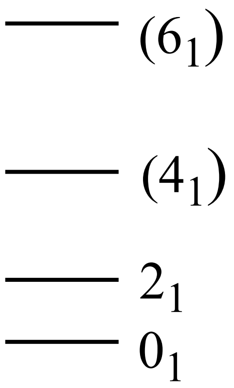

Level spacings ← different inertial functions

A. Gade et al., PRC103, 014314 (2021)

Washiyama & Yoshida, in preparation

Discussion : low-lying 0_2 state in N=40 isotones

^{60}Ca

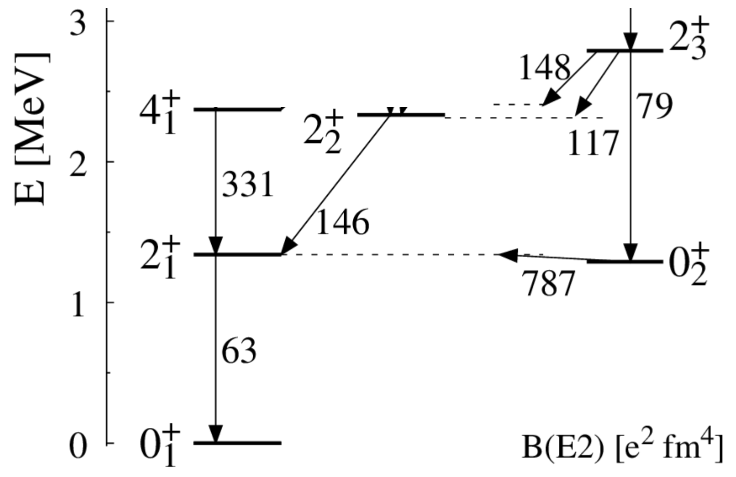

$R_{0/2}$ = 0.96

^{64}Cr

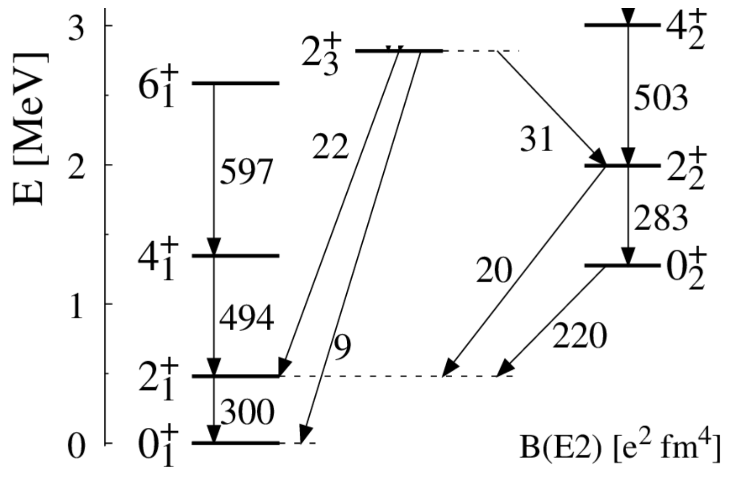

$R_{0/2}$ = 2.66

^{68}Ni

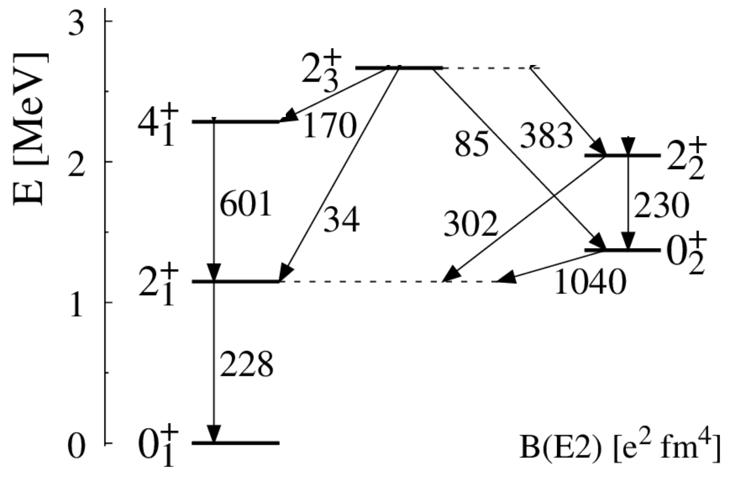

$R_{0/2}$ = 1.19

$R_{0/2} = E(0_2) / E(2_1)$

Low 0_2^+ energy → What is the origin?

Result: positive-parity low-lying spectra

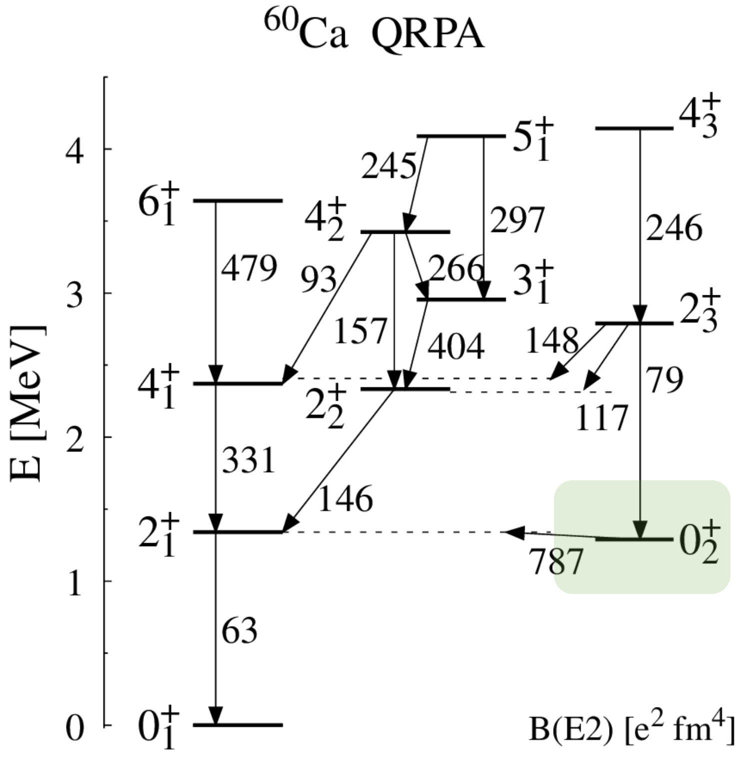

$$D_{\beta\beta} = D_{\gamma\gamma}/\beta^2 = D_k = D$$

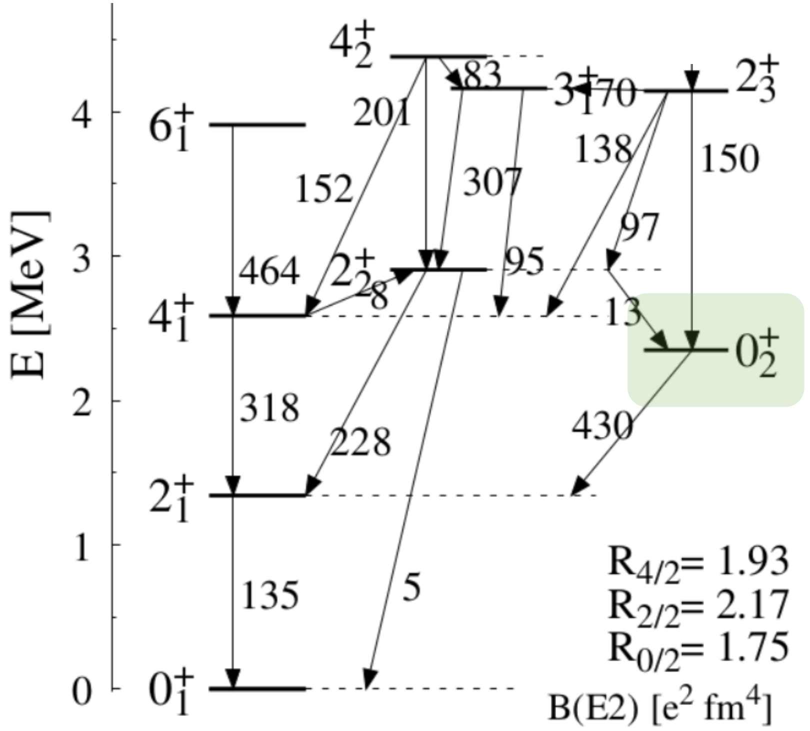

Inertial functions decreases the 0_2^+ energy

Inertial functions play an important role

Relation between QRPA and inertial functions

QRPA: linear response to an external field

Quadrupole
external field

$$\hat{F} = \sum_i^A r_i^2 Y_{2m}(\Omega_i)$$

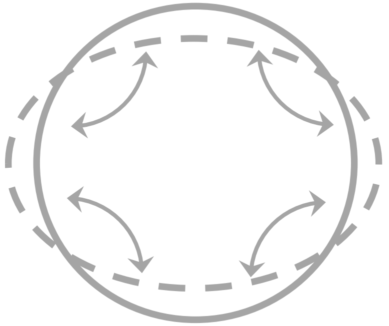

Response
(strength, frequency)

Inertia associated with
quadrupole moments

$$D_{\beta\beta},\ D_{\beta\gamma},\ D_{\gamma\gamma}$$

Result: potential energy surface in Cr isotopes

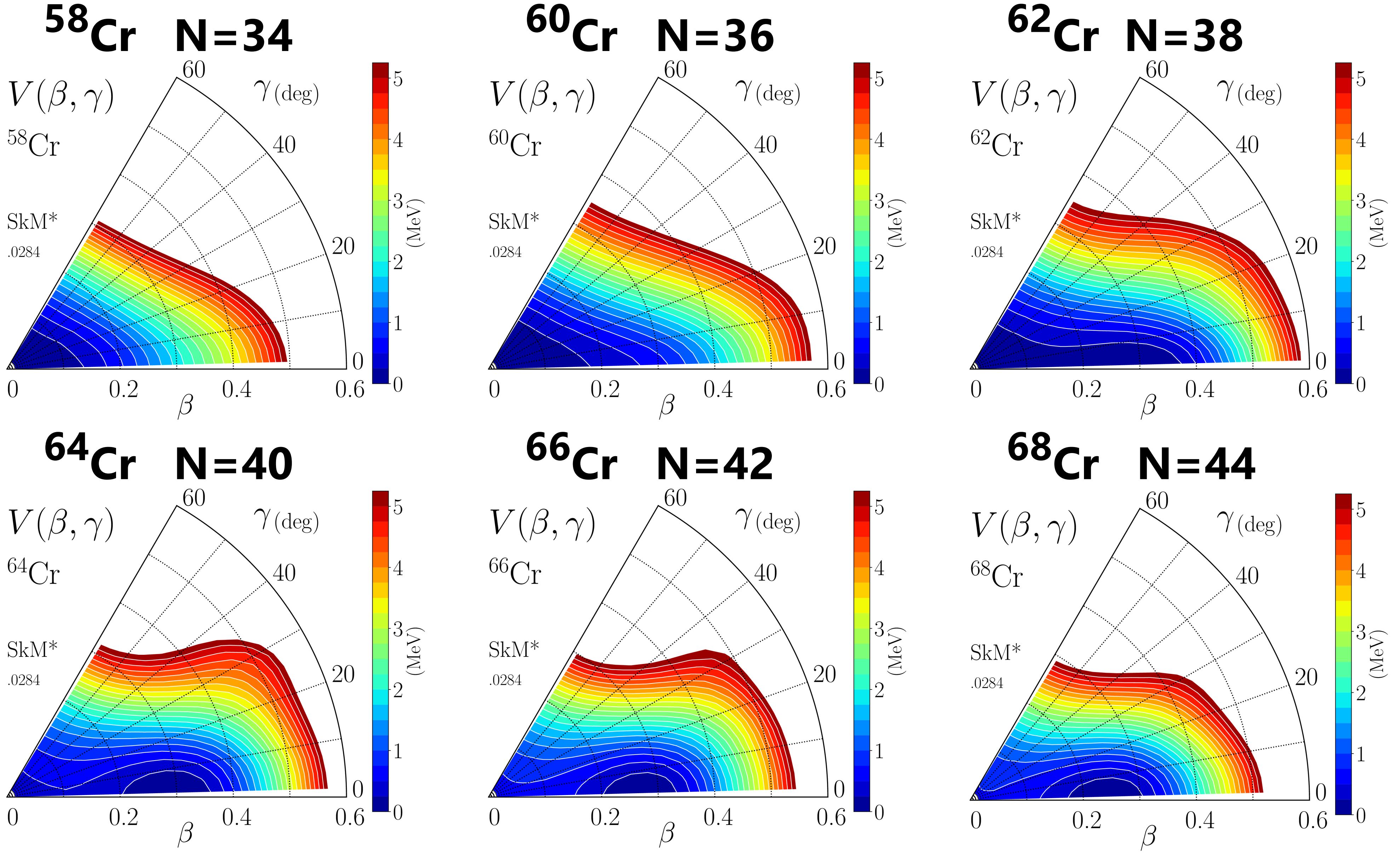

Spherical to prolate

Flat potential
→ Shape fluctuation

Systematics on B(E2; $0_1 \rightarrow 2_1$)

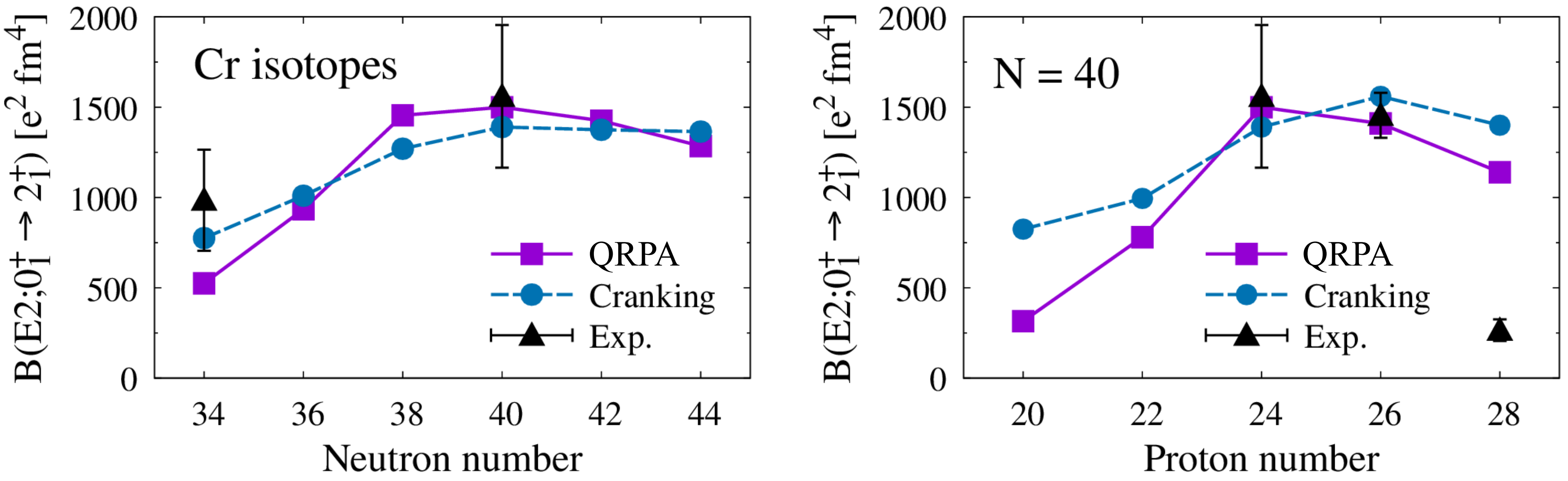

Good in ^{64}Cr (N=40)
Underestimate in ^{58}Cr (N=34)

Good in ^{64}Cr, ^{66}Fe
Overestimate in ^{68}Ni

Low 0_2 energy and dynamical shape coexistence

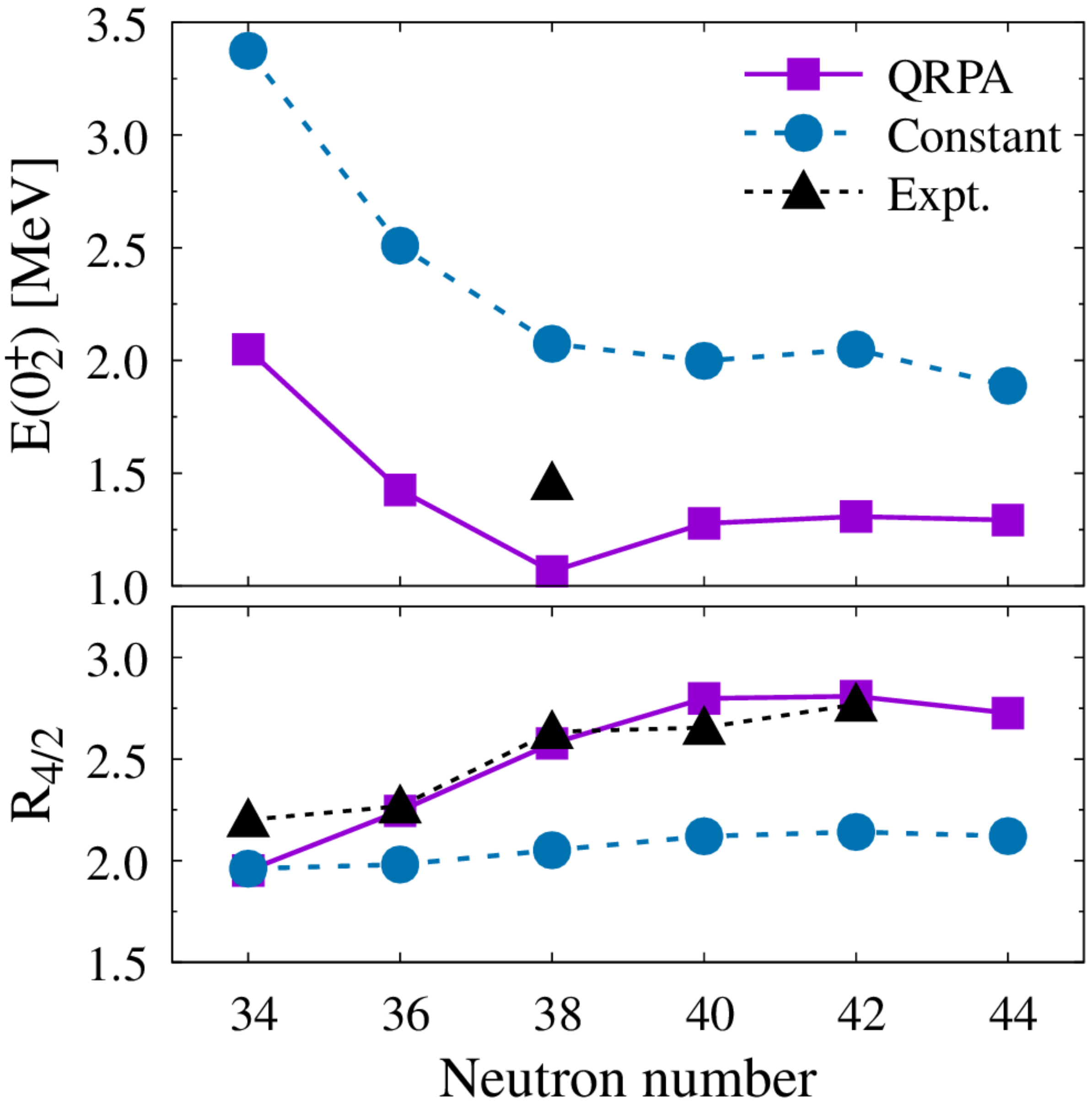

Cr isotopes

^{62}Cr: A. Gade et al., PRC103, 014314 (2021)

DFT + Cranking approximation

Prochniak et al., NPA730 (2004) 59;
Niksic et at., PRC79 (2009) 034303;
Delaroche et al., PRC81 (2010) 014303, etc.

Skyrme, Gogny, Relativistic, etc.

Low computation cost

Neglect dynamical effects (time-odd terms)

Adiabatic TDDFT

Dobaczewski, Skalski, NPA369,123(1981)

Perturbative cranking approximation

$$\mathcal{M}^{\mathrm{PC}} = \frac{1}{2}[M^{(1)}]^{-1} M^{(3)} [M^{(1)}]^{-1}$$

$$M_{ij}^{(n)} = \sum_{\mu<\nu} \frac{\langle \phi(\beta,\gamma)|\hat{Q}|\mu\nu\rangle\langle\mu\nu|\hat{Q}^\dagger|\phi(\beta,\gamma)\rangle}{(E_\mu + E_\nu)^n}$$

Ground state information

No dynamical effect

Q : Quadrupole moment operator

ϕ : constrained HFB state

E : quasiparticle energy

$$|\mu\nu\rangle = a_\mu^\dagger a_\nu^\dagger |\phi(\beta,\gamma)\rangle$$

Methods for inertial functions $D_{\beta\beta}, D_{\beta\gamma}, D_{\gamma\gamma}, \mathcal{J}_k$

DFT + Cranking approximation

Prochniak et al., NPA730 (2004) 59;
Niksic et at., PRC79 (2009) 034303;
Delaroche et al., PRC81 (2010) 014303, etc.

Skyrme, Gogny, Relativistic, etc.

Low computation cost

Neglect dynamical effects (time-odd terms)

Adiabatic TDDFT

Dobaczewski, Skalski, NPA369,123(1981)

Local QRPA

Hinohara et al., PRC82 (2010) 064313

Adiabatic SCC (self-consistent collective coordinate)

Matsuo, Nakatsukasa, Matsuyanagi, PTP103 (2000)

Include dynamical effects by QRPA

High computation cost

P + Q force, β–γ plane — Hinohara et al., PRC84 (2011) 061302; 85 (2012) 024323; Sato, Hinohara, NPA849 (2011) 53

Skyrme DFT, axial symmetry — Yoshida, Hinohara, PRC83 (2011) 061302

Our Method: Local QRPA with Skyrme DFT on β–γ plane

Pairing and collectivity: Special case in 60Ca?

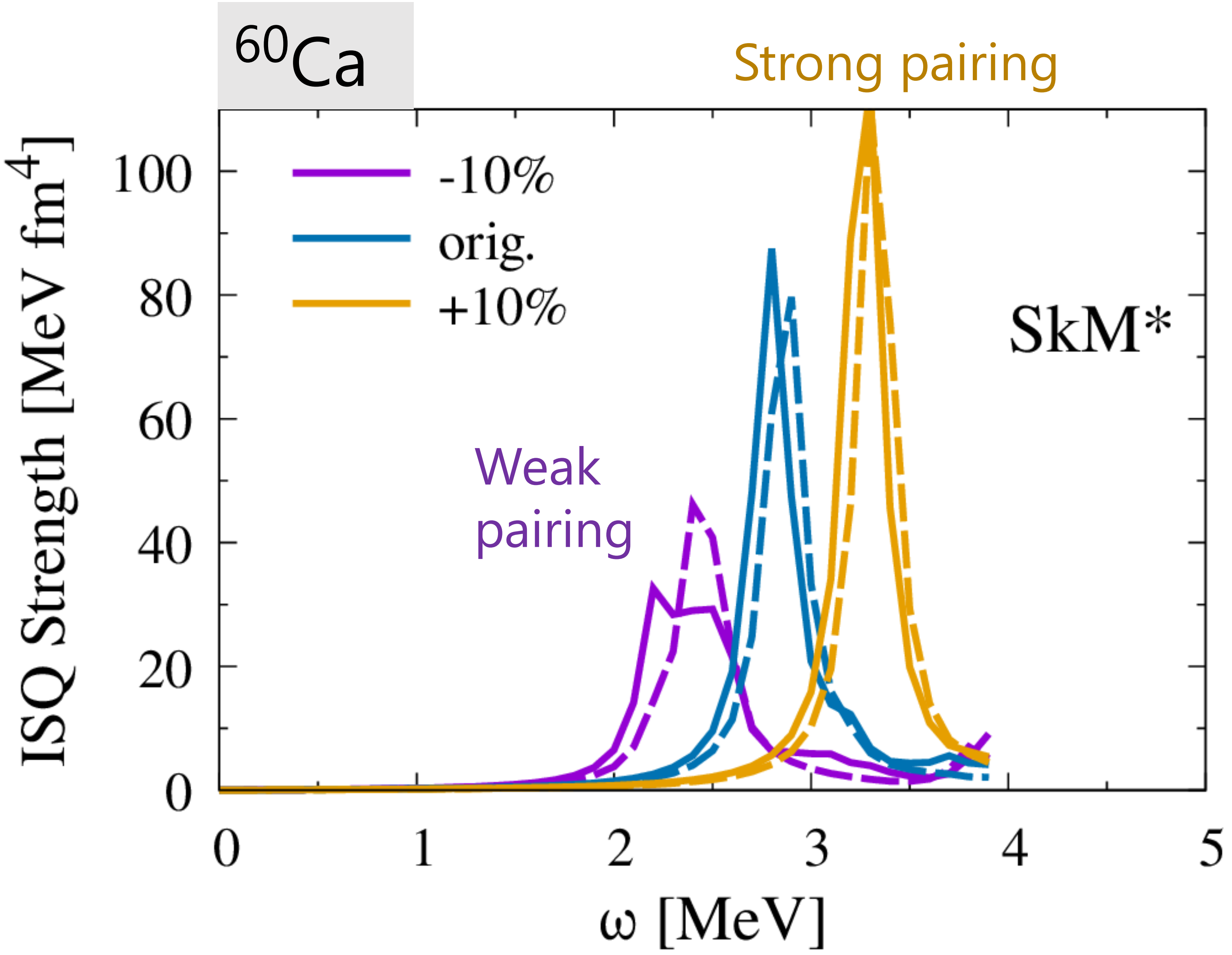

Pairing strength

Peak energy

Transition strength

Discussion: Pairing and quadrupole collectivity

When the pairing strength increases,

Potential would become soft against quadrupole deformation

➡ Quadrupole collectivity would be increased

Deformation would become small

➡ Quadrupole collectivity would be reduced

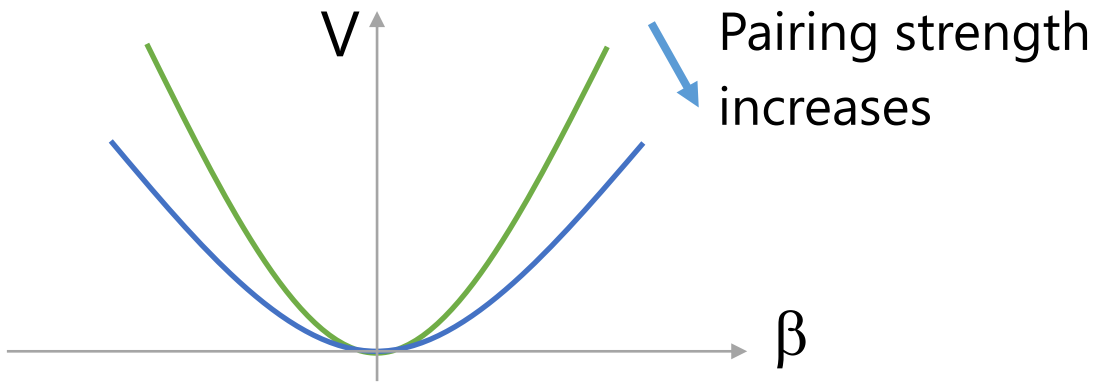

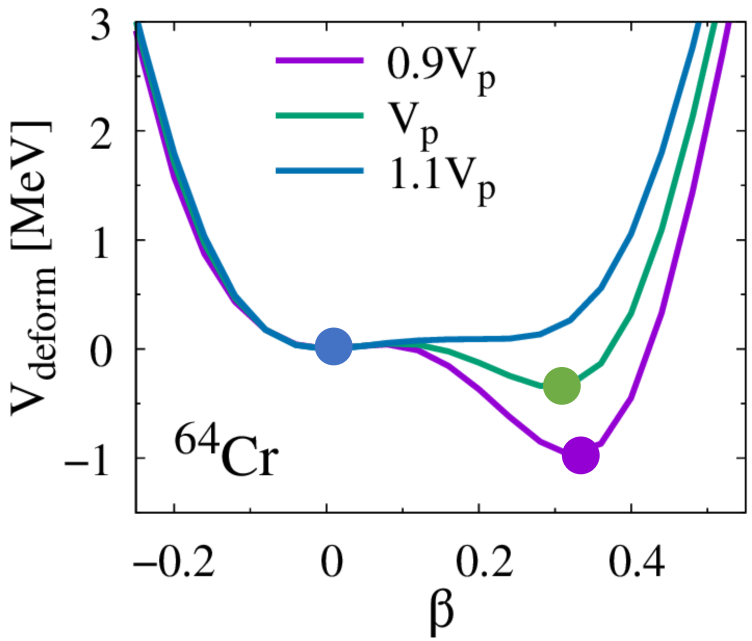

Discussion: Pairing and quadrupole collectivity

Yamagami & Giai, Phys. Rev. C 69, 034301 (2004)

Spherical QRPA calculations for the first excited state $I^{\pi} = 2_1^+$
in the N=20 gap in ^{32}Mg

When the pairing strength increases,

Two competing effects:

1. Increase pairing gap & quasiparticle (QP) energy
   → increase excitation energies if correlation is small
2. More 2QP configurations to the excited state and larger correlation
   → decrease excitation energy

Discussion: Pairing and quadrupole collectivity

Case 2 ^{32}Mg N=20

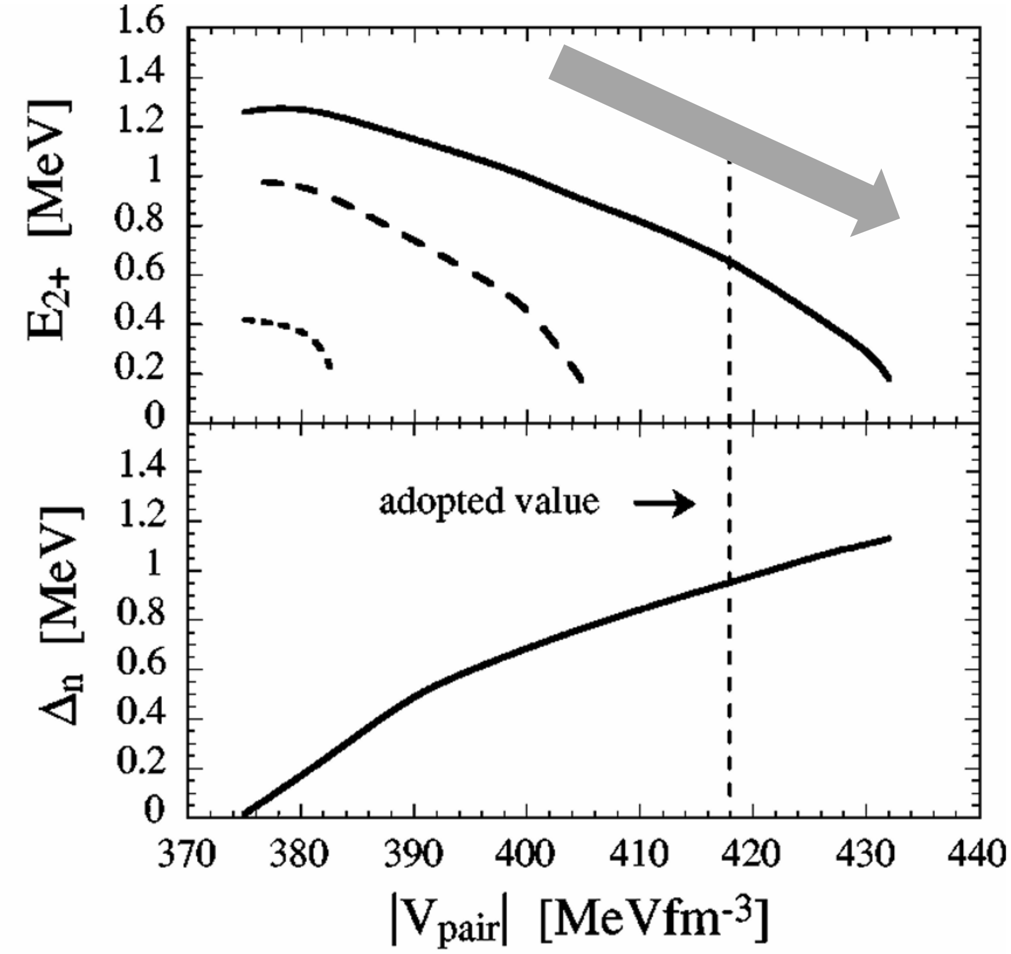

Yamagami & Giai, Phys. Rev. C 69, 034301 (2004)

2. More 2QP configurations to the excited state and larger correlation
   → decrease excitation energy

Result: Pairing and quadrupole collectivity

2_1 energy

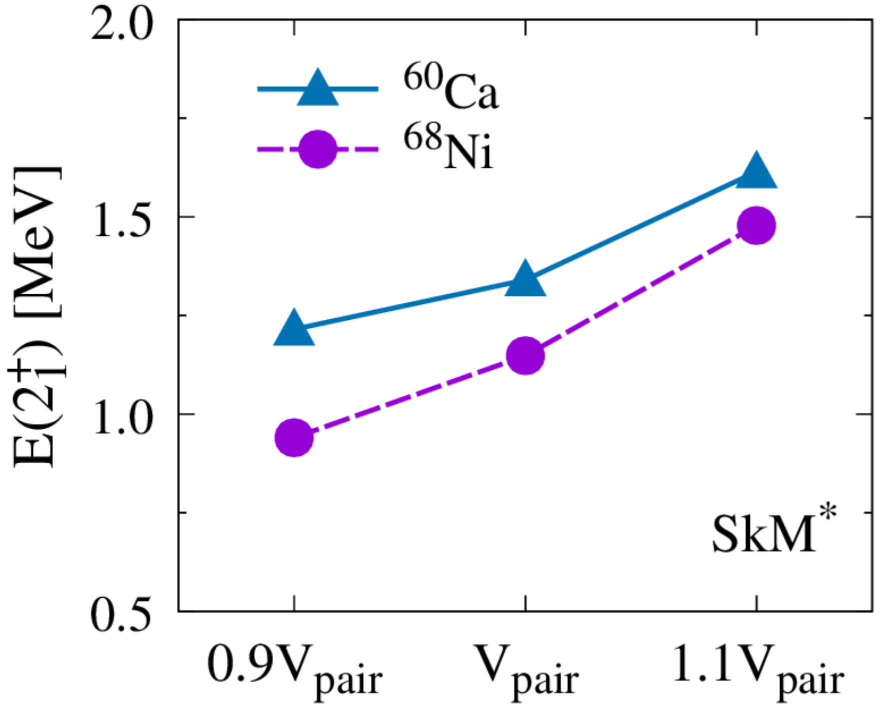

B(E2; $2_1 \rightarrow 0_1$) value

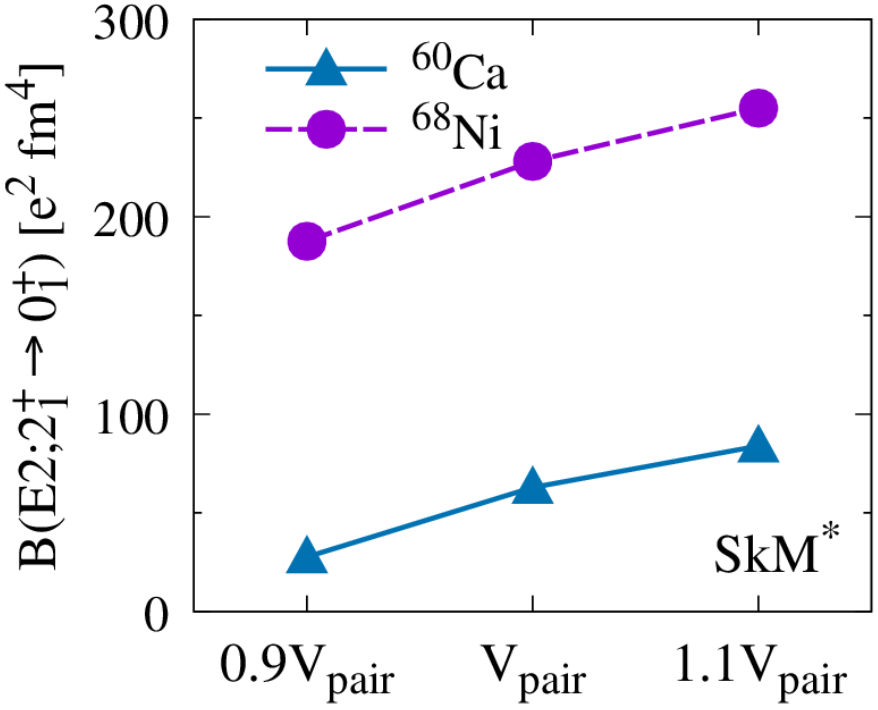

When the pairing strength increases,
both 2_1 energy and B(E2) increases.

Discussion: Role of parameters in the model

Simple harmonic oscillator and constant mass model assuming small amplitude limit (cf. Bohr-Mottelson)

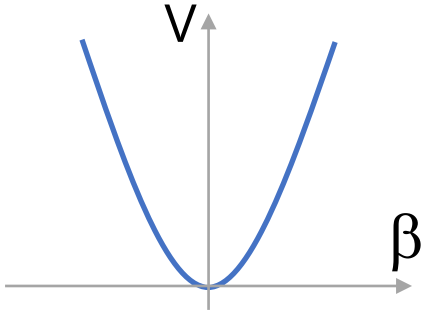

$$V(\beta,\gamma) = \frac{1}{2}C\beta^2$$

$$D_{\beta\beta} = D_{\gamma\gamma}/\beta^2 = D_1 = D_2 = D_3 = D$$
$$D_{\beta\gamma} = 0$$

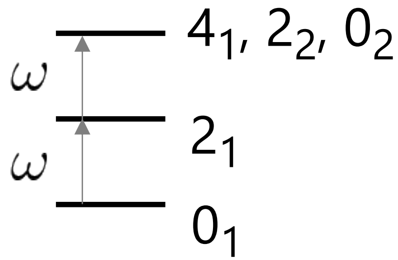

Excitation energy $\omega = \sqrt{\frac{C}{D}}$

Transition probability $B(E2; 2_1 \to 0_1) = \left(\frac{3ZeR^2}{4\pi}\right)^2 \frac{1}{2\sqrt{CD}}$ $R = 1.2A^{1/3}$ fm

$$\propto \frac{1}{D\omega}$$

Result: Curvature and mass

Curvature v.s. pairing strength

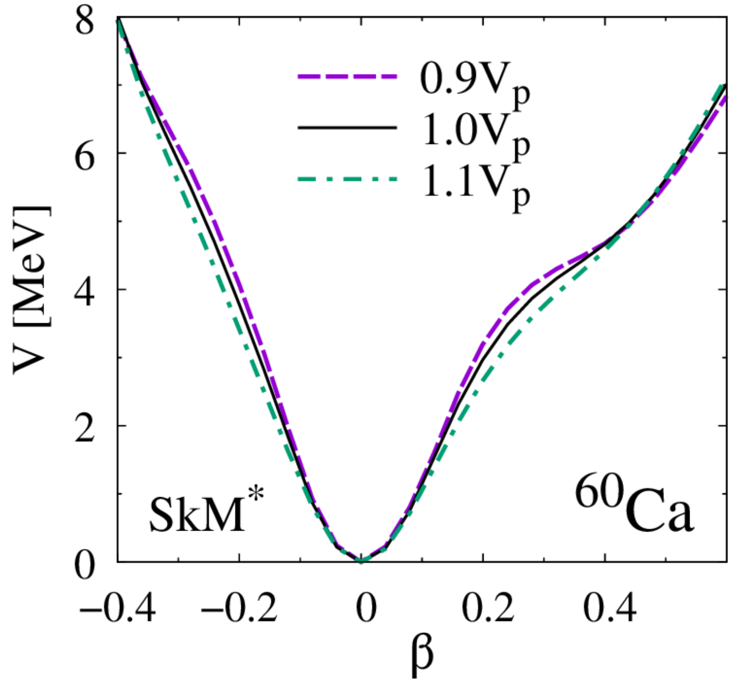

Mass v.s. pairing strength

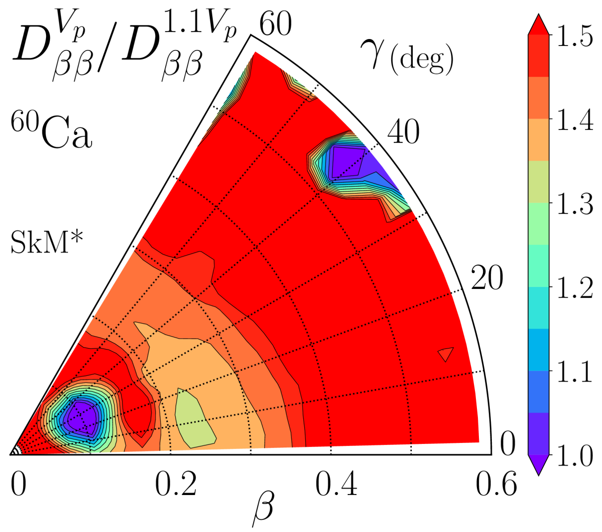

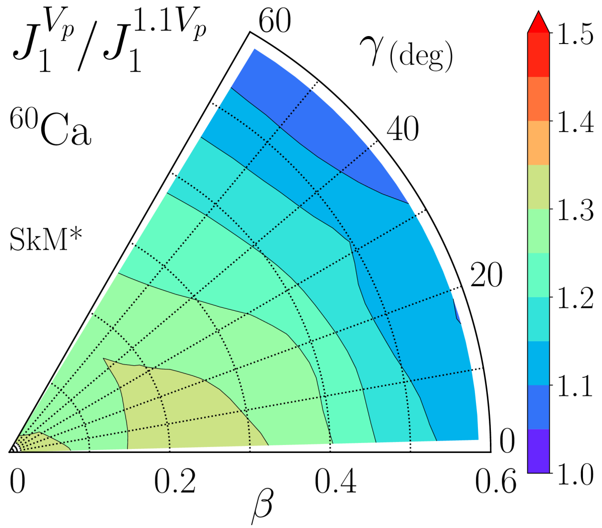

Stronger pairing, smaller C

≈10% change

Stronger pairing, smaller D

20%-50% change

Large change of mass = Large change of quadrupole collectivity

Calculation method: Local QRPA

Local QRPA at each CHFB state

$$\delta\langle\phi(s)|[\hat{H}_{\mathrm{M}}(s),\hat{Q}^i(s)]-\frac{1}{i}\hat{P}^i(s)|\phi(s)\rangle=0$$

$$\delta\langle\phi(s)|[\hat{H}_{\mathrm{M}}(s),\frac{1}{i}\hat{P}^i(s)]-C_i(s)\hat{Q}^i(s)|\phi(s)\rangle=0$$

s : deformation parameters

=

Hinohara et al., PRC82 (2010) 064313

$$\begin{pmatrix} A & B \\ B^* & A^* \end{pmatrix}\begin{pmatrix} Q^i \\ -Q^{i*} \end{pmatrix}=\frac{1}{i}\begin{pmatrix} P^i \\ -P^{i*} \end{pmatrix}$$

$$\begin{pmatrix} A & B \\ B^* & A^* \end{pmatrix}\begin{pmatrix} P^i \\ -P^{i*} \end{pmatrix}=iC_i\begin{pmatrix} Q^i \\ -Q^{i*} \end{pmatrix}$$

"local" indicates that QRPA is solved at each deformation

➡ Low-lying collective modes

Eigen-frequency $\hat{Q}^i,\ \hat{P}^i,\ C_i=\Omega_i^2$

➡ $M(s)$ ➡ $D_{\beta\beta},\ D_{\beta\gamma},\ D_{\gamma\gamma}$

$$\frac{\partial s_m}{\partial q^i}=\langle\phi(\beta,\gamma)|[\hat{s}_m,\frac{1}{i}\hat{P}_i]|\phi(\beta,\gamma)\rangle$$

$$M_{mn}(\beta,\gamma)=\sum_{i=1,2}\frac{\partial q^i}{\partial s_m}\frac{\partial q^i}{\partial s_n}$$

$$s_1=r^2Y_{20},\quad s_2=r^2(Y_{22}+Y_{2-2})/\sqrt{2}$$

Finite amplitude method (FAM)

Nakatsukasa et al., PRC76 (2007) 024318
Avogadro & Nakatsukasa, PRC84, 014314

✓ Small computational cost

✓ equivalent to QRPA response

Quadrupole collectivity and beyond-mean-field approach

Five-dimensional collective Hamiltonian (5DCH) method

$$\mathcal{H} = T_{\rm vib} + T_{\rm rot} + V(\beta,\gamma)$$

Vibrational mass

$$T_{\rm vib} = \frac{1}{2}D_{\beta\beta}(\beta,\gamma)\dot{\beta}^2 + D_{\beta\gamma}(\beta,\gamma)\dot{\beta}\dot{\gamma} + \frac{1}{2}D_{\gamma\gamma}(\beta,\gamma)\dot{\gamma}^2$$

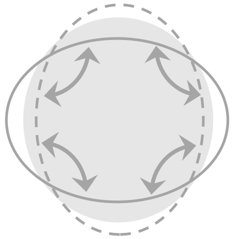

$$T_{\rm rot} = \frac{1}{2}\sum_{k=1}^{3}\mathcal{J}_k(\beta,\gamma)\omega_k^2$$

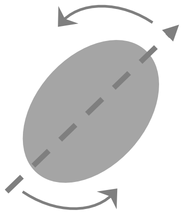

Moment of inertia

$V(\beta,\gamma)$	Constrained DFT
$D_{\beta\beta},\ D_{\beta\gamma},\ D_{\gamma\gamma},\ \mathcal{J}_k$	**DFT + Local QRPA**

Inertia ⟺ Quadrupole collectivity

LQRPA includes dynamical residual effects

Previous works ignore them

(Cranking approximation for inertia)

Washiyama, Hinohara, Nakatsukasa, Phys. Rev. C 109, L051301(2024)

Quadrupole collectivity and beyond-mean-field approach

Quantize 5DCH, collective Schrödinger equation

$$\hat{H}\Psi_{\alpha IM}(\beta,\gamma,\Omega) = E_{\alpha I}\Psi_{\alpha IM}(\beta,\gamma,\Omega)$$

I : Angular momentum
M : Its z-component in the laboratory frame
Ω : Euler angles (laboratory ↔ body-fixed frame)

▼

Excitation energies $E_{\alpha I}$, transition probability B(E2) between states

Computational cost

Time consuming part is computing $D_{\beta\beta}, D_{\beta\gamma}, D_{\gamma\gamma}$ in the β,γ plane

Computational time is ~60000 hours in 100 β,γ mesh points,
which was efficiently parallelized with OpenMP + MPI
in Wisteria/BDEC-01 Odyssey (Univ. Tokyo)

Skyrme energy density functional (EDF)

Skyrme EDF

Bender, Heenen, Reinhard, Rev. Mod. Phys. 75, 121 (2003)
Perlińska et al., PRC69, 014316 (2004)

$$\mathcal{E}_{\mathrm{Sk}} = \int d^3r \sum_{t=0,1} \mathcal{H}_t(\boldsymbol{r})$$

zero-range interaction

$$\mathcal{H}_t = C_t^{\rho}[\rho_0]\rho_t^2 + C_t^{\Delta\rho}\rho_t\Delta\rho_t + C_t^{\tau}\rho_t\tau_t + C_t^{\nabla\cdot J}\rho_t\nabla\cdot\boldsymbol{J}_t - C_t^{T}\sum_{\mu,\nu=x}^{z} J_{t,\mu\nu}J_{t,\mu\nu} - \frac{1}{2}C_t^{F}[(\sum_{\mu=x}^{z} J_{t,\mu\mu})^2 + \sum_{\mu,\nu=x}^{z} J_{t,\mu\nu}J_{t,\nu\mu}]$$

$$+ C_t^{s}[\rho_0]\boldsymbol{s}_t^2 + C_t^{\nabla s}(\nabla\cdot\boldsymbol{s}_t)^2 + C_t^{\Delta s}\boldsymbol{s}_t\cdot\Delta\boldsymbol{s}_t - C_t^{\tau}\boldsymbol{j}_t^2 + C_t^{\nabla\cdot J}\boldsymbol{s}_t\cdot\nabla\times\boldsymbol{j}_t + C_t^{T}\boldsymbol{s}_t\cdot\boldsymbol{T}_t + C_t^{F}\boldsymbol{s}_t\cdot\boldsymbol{F}_t$$

$$\rho_q(\boldsymbol{r}) = \rho_q(\boldsymbol{r},\boldsymbol{r}')|_{\boldsymbol{r}=\boldsymbol{r}'}, \quad \tau_q(\boldsymbol{r}) = \nabla\cdot\nabla'\rho_q(\boldsymbol{r},\boldsymbol{r}')|_{\boldsymbol{r}=\boldsymbol{r}'}, \quad J_{q,\mu\nu}(\boldsymbol{r}) = -\frac{i}{2}(\nabla_\mu - \nabla'_\mu)s_{q,\nu}(\boldsymbol{r},\boldsymbol{r}')|_{\boldsymbol{r}=\boldsymbol{r}'}$$

$$\boldsymbol{s}_q(\boldsymbol{r}) = \boldsymbol{s}_q(\boldsymbol{r},\boldsymbol{r}')|_{\boldsymbol{r}=\boldsymbol{r}'}, \quad \boldsymbol{T}_q(\boldsymbol{r}) = \nabla\cdot\nabla'\boldsymbol{s}_q(\boldsymbol{r},\boldsymbol{r}')|_{\boldsymbol{r}=\boldsymbol{r}'}, \quad \boldsymbol{j}_q(\boldsymbol{r}) = -\frac{i}{2}(\nabla - \nabla')\rho_q(\boldsymbol{r},\boldsymbol{r}')|_{\boldsymbol{r}=\boldsymbol{r}'}, \quad F_{\mu,q} = \frac{1}{2}\sum_{\nu=x}^{z}(\nabla_\mu\nabla'_\nu + \nabla'_\mu\nabla_\nu)s_{q,\nu}(\boldsymbol{r},\boldsymbol{r}')|_{\boldsymbol{r}=\boldsymbol{r}'}$$

$$\rho_{t=0} = \rho_n + \rho_p \qquad \rho_q(\boldsymbol{r},\boldsymbol{r}') = \sum_{\sigma=\pm1}\rho_q(\boldsymbol{r}\sigma,\boldsymbol{r}'\sigma)$$

$$\rho_{t=1} = \rho_n - \rho_p \qquad \boldsymbol{s}_q(\boldsymbol{r},\boldsymbol{r}') = \sum_{\sigma,\sigma'=\pm1}\rho_q(\boldsymbol{r}\sigma,\boldsymbol{r}'\sigma')\langle\sigma'|\hat{\boldsymbol{\sigma}}|\sigma\rangle$$

Pairing EDF

$$\mathcal{E}_{\mathrm{pairing}} = \int d^3r \sum_{q=p,n} \mathcal{H}_q(\boldsymbol{r})$$

$$\mathcal{H}_q(\boldsymbol{r}) = \frac{V_q}{4}\left[1 - \frac{\rho_0(\boldsymbol{r})}{\rho_c}\right]\tilde{\rho}_q(\boldsymbol{r})\tilde{\rho}_q^*(\boldsymbol{r})$$